ImmunoHorizons

RESEARCH ARTICLE

Innate Immunity

Erdr1 Drives Macrophage Programming via Dynamic Interplay with YAP1 and Mid1

Yuhang Wang

Department of Microbiology and Immunology, University of Iowa, IA City, IA

ABSTRACT

Erythroid differentiation regulator 1 (Erdr1) is a stress-induced, widely expressed, highly conserved secreted factor found in both humans and mice. Erdr1 is linked with the Hippo-YAP1 signaling. Initially identified as an inducer of hemoglobin synthesis, Erdr1 emerged as a multifunctional protein, especially in immune cells. Although Erdr1 has been implicated in regulating T cells and NK cell function, its role in macrophage remains unclear. This study explored the function and mechanism of Erdr1 in macrophage inflammatory response. The data demonstrated that Erdr1 could promote anti-inflammatory cytokine production, a function that also has been reported by previous research. However, I found Erdr1 also could play a proinflammatory role. The function of Erdr1 in macrophages depends on its dose and cell density. I observed that Erdr1 expression was inhibited in M1 macrophages but was upregulated in M2 macrophages compared with unpolarized macrophages. I hypothesized that Erdr1 balances the inflammatory response by binding with distinct adaptors dependent on varying concentrations. Mechanistically, I demonstrated YAP1 and Mid1 as the two adaptor proteins of Erdr1. The Erdr1–YAP1 interaction promotes anti-inflammatory cytokine production when Erdr1 levels are elevated, whereas the Erdr1–Mid1 interaction induces proinflammatory cytokine production when Erdr1 levels are decreased. This study highlights the effects of Erdr1 on regulating cytokine production from polarized macrophages potentially by regulating YAP1 in the nonclassical Hippo pathway. *ImmunoHorizons*, 2024, 8: 198–213.

INTRODUCTION

Erdr1 was initially identified as a stress-induced factor that acts as a hemoglobin synthesis-inducing factor in leukemia cells and is highly conserved between humans and mice (1, 2). Subsequent research has been demonstrated to highlight its important role in immune response (3–6). Erdr1 has been shown to play a critical role in T cell proliferation, activation (3, 4), and apoptosis (5). Recombinant Erdr1 protein treatment strengthens TCR signal in T cells by enhancing calcium influx (3) and PLCγ1 signaling (4) upon activation by CD3 Ab in vitro. In vivo, it significantly promotes thymocyte proliferation (3). However, Erdr1 has also been found to promote Treg cell activation (7), and endogenous overexpression of Erdr1 induces T cell apoptosis upon activation (5). The conflicting functions of Erdr1 on T cells are most likely due to the Erdr1 concentration and cell context. Apart from T cells, Erdr1 protein has also been shown to boost NK cell activation by promoting F-actin accumulation (6). Additionally, Erdr1 has been implicated in the pathogenesis of inflammatory disorders such as psoriasis (8) and rosacea (9). Notably, Erdr1 was downregulated in these patients and has a negative correlation with the proinflammatory cytokine IL-18 (9, 10), a readout cytokine of the inflammasome (11, 12). Animal experiments have manifested the broadly anti-inflammatory effect of Erdr1 protein in treating inflammatory disorders such as psoriasis (10), rosacea (9), colitis (13), and arthritis (7). Erdr1 has also been reported to play a negative role in macrophage migration (14). However, the precise function and mechanism of Erdr1 in macrophages remain largely unexplored. I noted that Erdr1 was upregulated in anti-inflammatory macrophages and

Received for publication January 29, 2024. Accepted for publication February 6, 2024.

Address correspondence and reprint requests to the current address: Yuhang Wang, Department of Pathology, University of Iowa, Iowa City, IA 52242. E-mail address: yuhang-wang@uiowa.edu

ORCID: 0009-0008-9915-9121 (Y.W.).

This work was supported by National Institutes of Health Grant P01 AI060699.

Abbreviations used in this article: BMDM, bone marrow–derived macrophage; HA, hemagglutinin; qPCR, quantitative PCR.

The online version of this article contains supplemental material.

https://doi.org/10.4049/immunohorizons.2400004

ImmunoHorizons is published by The American Association of Immunologists, Inc.

downregulated in proinflammatory macrophages compared with naive macrophages. The preliminary data suggested that Erdr1 exhibits a dose-dependent, bell-shaped effect on the macrophage inflammatory response. I propose that Erdr1 performs this role by interacting with different adaptor proteins, enabled by alterations in its structure triggered by fluctuating concentrations. I aim to investigate the candidate adaptors of Erdr1 and uncover the mechanism of Erdr1 in macrophages.

Previous research has demonstrated that secreted Erdr1 mediates cellular adaptation; it promotes cell survival at low concentrations and low cell density but enhances cell death at high concentrations and high cell density (1), indicating that Erdr1 is involved in maintaining cellular homeostasis. Moreover, Erdr1 has been shown to exhibit conformational changes at the sites of cell–cell contact (1). Contact inhibition is a mechanism that regulates cell proliferation by modulating the Hippo-YAP1 signaling pathway (15–17). These findings suggest that Erdr1 may be associated with YAP1. Furthermore, I have discovered a strong correlation between Erdr1 and YAP1 in previous studies (5, 18–21). Firstly, Erdr1 has been found to directly regulate YAP1 signaling. For instance, in T cells, the overexpression of Erdr1 augments the expression of YAP1 and its signature gene (Amotl1) following T cell stimulation (5). Secondly, YAP1 knockout has been shown to affect Erdr1 expression. In Treg cells, YAP1 knockout prominently upregulates Erdr1 upon stimulation (19), and similarly, YAP1 knockout leads to a remarkable increase in Erdr1 expression in Müller glia cells during degeneration induction (20). Meanwhile, the knockout of YAP1 in mouse incisor epithelium leads to a significant downregulation of Erdr1 (18). Given the robust correlation between Erdr1 and YAP1, I hypothesized that YAP1 is one of the adaptors of Erdr1.

The preliminary data demonstrated that Erdr1 has a strong interaction with YAP1 in the cytoplasm in anti-inflammatory but not in proinflammatory macrophages. I predicted Erdr1 drives an anti-inflammatory state by directly interacting with YAP1 and can also promote macrophage proinflammatory reprogramming by disconnecting with YAP1 and binding to Mid1, another candidate adaptor of Erdr1. Mid1 is a highly conserved gene expressed ubiquitously in humans and mice (22). Initially identified for its essential role in development (22), Mid1 has also been shown to play a crucial role in macrophage activation (23–25). My hypothesis is based on several lines of evidence. Firstly, Erdr1 and Mid1 are closely linked in gene mapping, because they are neighboring genes located in the PAR region of the sex chromosomes X and Y in mice (26–28). Secondly, previous studies have established a functional connection between Mid1 and both Erdr1 (19, 29–46) and YAP1 (19, 47, 48), as well as YAP1 downstream genes such as CTGF (49), Cry61 (29, 34, 38, 49), and IL-1β (25, 30, 49). Thirdly, Erdr1 and Mid1 are known to play a shared role in regulating YAP1 signature gene expression (30, 49, 50). Fourthly, Mid1 is a zinc finger protein with three zinc finger domains and multiple zinc-binding sites that are critical for its function. Erdr1 contains the HESTH sequence (118–122), representing a potent zinc-binding motif known as HEXXH (51). Notably, Erdr1 and Mid1 are involved in dysregulated intracellular zinc signaling (32). They are likely involved in intracellular zinc mobilization through the formation of an Erdr1–Mid1 zinc channel. Overall, the hypothesis posits that Erdr1 dual-regulates the macrophage inflammatory response through dynamic interactions with YAP1 and Mid1. As an intrinsically disordered protein (52), Erdr1 lacks a fixed structure and has the potential to play multiple functions by dynamically and cooperatively binding to partners.

Mechanistically, I demonstrate that Erdr1 dynamically modulates macrophage inflammatory response by interacting with YAP1 and Mid1 through distinct domains. Upregulated Erdr1 sequesters YAP1 directly in the cytoplasm and drives macrophage proinflammatory response. Conversely, downregulated Erdr1 primes the macrophage anti-inflammatory response by disconnecting from YAP1 and interacting with Mid1. More importantly, this study highlights the effects of Erdr1 on regulating cytokine production from polarized macrophages potentially by regulating YAP1 in the nonclassical Hippo pathway.

MATERIALS AND METHODS

Cell culture

293T and HeLa cells were cultured with DMEM in the presence of 10% FBS, 100 IU/ml penicillin, and 100 μg/ml streptomycin. RAW246.7 were cultured with RPMI 1640 medium in the presence of 10% FBS, 100 IU/ml penicillin, and 100 μg/ml streptomycin.

Mouse bone marrow–derived macrophages

C57BL/6 mice were killed, and the femurs were removed. Bone marrow was harvested by flushing with bone marrow–derived macrophage (BMDM) medium (RPMI 1640 medium supplemented with 10% FBS, antibiotics, L-glutamine, and 10 μg/ml M-CSF). The harvested cells were centrifuged at 300*g* for 10 min and were treated with ACK lysis buffer (ThermoFisher, A1049201) for 1 min to remove RBCs. ACK lysis buffer was neutralized by adding 10 volumes of PBS, and the cells were spun down at 300*g* for 10 min. The pelleted cells were resuspended in BMDM medium and were plated at 0.6×10^6 cells/ml for culture. The medium was replaced on days 4, 5, and 6 of culture before cell use on day 7. In some experiments, BMDMs were treated with indicated concentrations of LPS, IL-4, or purified Erdr1 proteins. Some experiments seed different cell densities as indicated. All animal studies were approved by the University of Iowa Animal Care and Use Committee and meet stipulations of the Guide for the Care and Use of Laboratory Animals.

Plasmid preparation and transduction

Full-length Erdr1 (Erdr1–177) and Erdr1 deficiency C-terminal 32 amino acids (Erdr1–145) with C-terminal hemagglutinin (HA) tags was synthesized (GenScript) and cloned into pcDNA3.1 plasmid using In-Fusion cloning (Clontech). YAP1 and Mid1 with C-terminal Flag were synthesized (GenScript) and cloned into pcDNA3.1 plasmid using In-Fusion cloning (Clontech). Plasmids

were sequenced before use. For transient expression, the plasmids were transfected into 293 T cells or HeLa cells using Lipofectamine 3000 transfection reagent (Life Technologies) according to the manufacturer's instructions. Lentiviral vectors were prepared as follows: For gene knockout, Erdr1, Mid1, and YAP1 Crispr/Cas9 knockout transfer plasmid were purchased from GenScript. For Erdr1 overexpression, full-length Erdr1 (Erdr1–177) C-terminal HA tags were cloned into pHAGE vector. Lentivirus was produced by transferring lentiviral vectors (transfer plasmid, psPAX2, and pMD2.G) into 293T cells following transfection protocol. Once produced, lentivirus was used for infection macrophage with different multiplicities of infection.

Cell viability assay

Cell viability was assessed by MTT assay. The MTT assay kit was purchased from Abcam (ab211091), and the assays were performed according to the manufacturer's protocol.

Coimmunoprecipitation assay

Cells were harvested with ice-cold PBS. Cell pellets were then lysed in immunoprecipitation buffer (IP lysis buffer: 25 mM Tris-HCl [pH 7.4], 150 mM NaCl, 1 mM EDTA, 1% Nonidet P-40, and 5% glycerol, 1 mM DTT, and 1 × protease/phosphatase inhibitors) for 30 min on ice and cleared by centrifugation at 13,000*g* for 15 min. The Erdr1-HA + YAP1-Flag or Erdr1-HA + Mid1-Flag was immunoprecipitated by anti-Flag M2 magnetic beads for 2 h, rotating end over end at 4°C. After the beads were pelleted and washed three times with IP lysis buffer, the immunocomplexes containing the Flag-tagged interaction protein were then prior to elution with 2× SDS sample buffer for 5 min at 95°C, followed by immunoblotting analysis.

Recombinant Erdr1

Generation of recombinant Erdr1 was performed by following protocol. Briefly, Erdr1–177 and Erdr1–145 with C-terminal His tag was cloned into the pET28a vector. *Escherichia coli* was transformed with this plasmid and cultured in medium containing ampicillin. Isopropyl β-D-thiogalactoside was introduced for protein induction. Erdr1–177-His and Erdr1–145-His were purified on a nickel column, and purity was >95% as confirmed by SDS-PAGE and immunoblotting. Potential endotoxin was removed using high-capacity endotoxin-removing spin columns (88274, ThermoFisher).

Anti-Erdr1 polyclonal Ab

Anti-Erdr1 peptide Ab (36–51 amino acids of Erdr1, N-RAPR PPRHTRHTRHTR-C) was received as a gift from Dr. June Round at Utah University (5). Erdr1-neutralizing Abs were received as a gift from Dr. Timothy L. Denning (13).

Immunofluorescence

The cells were seeded into 24-well plates containing 12-mm coated coverslips (Platinum Line). After the indicated culture or treatment times, the cells were fixed by incubation with PBS containing 4% (w/v) paraformaldehyde (Merck, catalog no. 104005100) for 15 min at room temperature. After washing three times with PBS for 5 min, the fixed cells were blocked and permeabilized by incubation with 500 μl of methanol for 5 min. PBS containing 5% (w/v) horse serum (Sigma, catalog no. A7906) were used for blocking for 1 h at room temperature. Primary Abs (Supplemental Table I) were diluted in 5% (w/v) horse serum/PBS and applied to coverslips and incubated at 4°C overnight. After three washes with PBS, the coverslips were incubated with secondary Ab diluted in 5% (w/v) horse serum/PBS at room temperature for 1 h. The cells were washed three times with PBS. The cells were stained nucleic and mounted onto glass slides using antifade mounting medium with DAPI (Vectashield). The slides were viewed using a Zeiss LSM 710 confocal microscope.

Immunoblotting

Total cell extracts were lysed using radioimmunoprecipitation assay buffer, which was supplemented with Complete mini protease inhibitor cocktail and phosphatase inhibitor cocktail from Roche. The lysates were put on ice for a period of 30 min and vortexed every 5 min. Following centrifugation at 15,000 rpm for 15 min at 4°C, the supernatants were collected. The proteins were resolved on a SDS polyacrylamide gel and transferred to a 0.45-μm polyvinylidene difluoride membrane. For immunoblot analysis, the indicated primary Abs were used and listed in Supplemental Table I and were used at 1,000-fold dilution. HRP-conjugated secondary Abs were used depending on the host species of the primary Abs.

Intracellular free zinc detection

Detecting intracellular zinc by using a commercial zinc indicator (FluoZin–3-acetoxymethyl ester; Invitrogen catalog no. F24195). In brief, RAW246.7 cells were cultured in 96-well plates with 0.6×10^6 cells/ml and cultured overnight. I washed the cells with PBS twice and then treated them with 1 μg/ml LPS, 10 μM $ZnCl_2$, the indicated Erdr1 protein, and 1 μM FluoZin–3-acetoxymethyl ester in serum-free medium. The, I measured the fluorescence (excitation/emission, 494/516) at the indicated time points with a well plate reader.

Cytokines quantification

IL-1β quantification was performed by harvesting cell supernatants at the indicated time points and treatment and assaying for IL-1β levels using a mouse IL-1β ELISA kit (DY401-050), according to the manufacturer's protocol.

Quantitative PCR and primers

Total RNA was extracted from macrophages at the indicated time points and treatment using TRIzol reagent (Invitrogen). Then 2 μg of RNA were used for cDNA synthesis, and 2 μl of cDNA were added to 23 μl of PCR mixture containing 2× SYBR Green Master Mix (ABI) and 0.2 μM of forward and reverse primers. Amplification was performed in an ABI

Prism 7500 thermocycler. The genes and forward and reverse primers are shown in Supplemental Table II. Cycle threshold (Ct) values were normalized to those of the housekeeping gene β-actin by the following equation: ΔCt = Ct (gene of interest) − Ct (β-actin). All results are shown as a ratio to β-actin calculated as 2 − (ΔCt).

Statistics

The *p* values of dynamic intracellular free zinc mobilization were determined by two-way ANOVA as specified in the figure legends. A Student *t* test was used to analyze differences in mean values between groups. All results are expressed as means ± SD. The *p* values less than 0.05 were considered statistically significant: $*p < 0.05$, $**p < 0.01$, $***p < 0.001$, and $****p < 0.0001$.

RESULTS

Erdr1 is distinctly regulated in macrophage proinflammatory and anti-inflammatory response

Macrophages can be polarized into proinflammatory M1 macrophages and anti-inflammatory M2 macrophages by different inducers (53, 54). I first investigated whether Erdr1 regulation occurs during the macrophage polarization process. To induce polarization, I treated M0 macrophages (bone marrow–derived macrophages [BMDMs]) with 1 μg/ml of LPS for 24 h to obtain M1 macrophages or with 20 ng/ml of IL-4 for 24 h to derive M2 macrophages. I confirmed M1 marker genes (IL-1β, IL-6, and TNF) and M2 marker gene (IL-10 and TGFβ) expression by quantitative PCR (qPCR) (data not shown). I noted a significant reduction in Erdr1 expression in M1 macrophages (Fig. 1A, 1B; Supplemental Fig. 1A), whereas it was markedly increased in M2 macrophages (Fig. 1A, 1B), compared with M0 macrophages. Further, I investigated the secretion and accumulation of Erdr1 in the supernatant of M1 and M2 macrophages. Immunoblot analysis showed a substantial increase of Erdr1 presence in the supernatant of M2 macrophages when compared with M0 macrophages (Fig. 1B). Interestingly, a significant elevation in Erdr1 levels was also observed in the supernatant of M1 macrophages (Fig. 1A, 1B; Supplemental Fig. 1A), despite the decrease in endogenous Erdr1 expression. Given that Erdr1 is known to be rapidly released from cells under stress through blebs or vesicles (1, 2), the increased secretion of Erdr1 in the medium of M1 macrophages might represent a mechanism to swiftly reduce intracellular Erdr1 levels rather than being an indicator of induced expression. I further examined the subcellular localization of Erdr1 in the polarized macrophage, employing immunofluorescence techniques. My findings reveal Erdr1 has an increased nuclear localization ratio in M1 macrophage but an increased cytoplasm localization ratio in M2 macrophage compared with the M0 macrophage (Fig. 1C). ImageJ analysis confirmed these findings (Fig. 1D). These observations suggest that Erdr1 displays distinct expression and localization patterns in M1 and M2 macrophages, indicating that Erdr1 may have dual roles in the inflammatory responses of macrophages.

Erdr1 exhibits a dose-dependent bell-shaped effect on LPS-induced IL-1β production in macrophages

IL-1β is one of the most important proinflammatory cytokines induced in M1 macrophages (53, 54). IL-1β is processed during the inflammasome activation process, similarly to IL-18 (11, 12). Erdr1 has been shown to have a negative correlation with IL-18 (55). I further aimed to elucidate the function of Erdr1 in regulating IL-1β production in M1 macrophages. Because I observed that Erdr1 exhibits both endogenous regulation and induced secretion during macrophage activation, I conducted experiments to investigate how intrinsic and extrinsic Erdr1 affect the production of IL-1β in response to LPS stimulation.

First, I assessed the endogenous Erdr1 function in LPS-induced IL-1β production. M0 macrophages were genetically modified to either knock out or overexpress Erdr1 through transduction with Erdr1 CRISPR/Cas9 knockout or Erdr1 overexpression lentiviruses, respectively, and I confirmed Erdr1 expression by qPCR (Fig. 2A, 2D). I observed that Erdr1 knockdown significantly suppressed LPS-induced IL-1β production (Fig. 2B, 2C). Interestingly, I observed that moderate overexpression of Erdr1 (Erdr1 OE1, ∼4.3-fold higher) dramatically enhanced LPS-induced IL-1β production, whereas a high-level overexpression of Erdr1 (Erdr1 OE2, ∼28.6-fold higher) inhibited LPS-induced IL-1β production (Fig. 2E, 2F). I discovered a bell-shaped correlation between the endogenous Erdr1 and IL-1β production (Fig. 2G), suggesting that Erdr1 plays a dual role in regulating IL-1β production.

Subsequently, I investigated the impact of secreted Erdr1 in the medium on LPS-induced IL-1β production. To achieve this, I employed a range of concentrations of an Erdr1 neutralization Ab to block the secreted Erdr1 in the medium. Interestingly, I observed a bell-shaped relationship between the Erdr1 Ab concentration and IL-1β production (Fig. 2H). These results suggest that an optimal concentration of Erdr1 in the medium exerts a positive effect in promoting IL-1β production. However, an excessive accumulation of Erdr1 in the medium appears to trigger a negative feedback mechanism, ultimately inhibiting IL-1β production.

Because purified Erdr1 protein has been shown to have an anti-inflammatory function (8, 9, 56). I next tested the effect of Erdr1 protein on IL-1β production in macrophages. Purified full-length Erdr1 was prepared and added to the medium in a series of concentrations as indicated. The data demonstrated that Erdr1 protein exhibits a dose-dependent bell-shaped effect on regulating LPS-induced IL-1β production (Fig. 2I). These findings provide striking evidence that a low dose of Erdr1 in the medium could enhance IL-1β production, whereas a high dose of Erdr1 inhibits IL-1β production. These results suggest that Erdr1's role in IL-1β production is closely correlated with its dosage.

https://doi.org/10.4049/immunohorizons.2400004

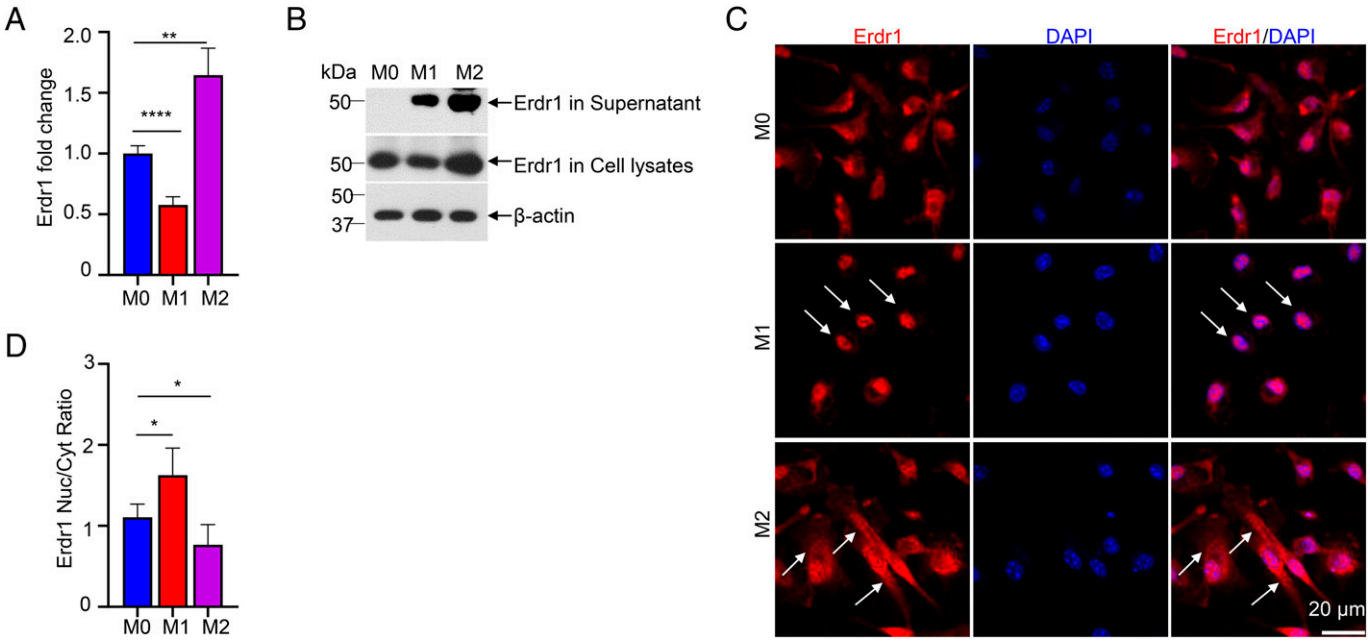

FIGURE 1. Erdr1 is distinctly regulated in M1/M2 macrophages.

The M0 macrophage used in this study was BMDM. The cell was seeded with a density of 0.6 × 10^6 cells/ml in 24-well plates. M0 macrophage was induced into M1 macrophage by treating with 1 μg/ml LPS for 24 h or into M2 macrophage by treating with 20 ng/ml IL-4 for 24 h. The same experiments were also conducted and got repeatable results in RAW246.7 cell. (**A**) qPCR analysis of Erdr1 mRNA expression in M0, M1, and M2 macrophages, qPCR normalized to β-actin expression ($n = 4$). (**B**) Immunoblot analysis of Erdr1 level in cell lysates and supernatant of M0, M1, and M2 macrophages with β-actin as the internal control. (**C**) Immunofluorescence staining of Erdr1 in M0, M1, and M2 macrophage and counterstained by DAPI. The white arrows in the M1 macrophage display Erdr1 are mainly localized in nucleus. The white arrows in the M2 macrophage display Erdr1 are mainly localized in the cytoplasm. Scale bar, 20 μm. (**D**) Erdr1 nuclear to cytoplasm (Neu/Cyt) intensity ratio was quantified by ImageJ based on immunostaining. $n = 5$ with more than 10 macrophages were analyzed per sample. The data represent mean ± SD. *$p < 0.05$, **$p < 0.01$, ****$p < 0.001$. The data are representative of at least three independent experiments.

In summary, my data reveal that Erdr1 can inhibit proinflammatory cytokines production, which has been reported. However, to my knowledge, I demonstrate for the first time that Erdr1 also has the potential to promote proinflammatory cytokine production. These findings suggest that Erdr1's influence on IL-1β production follows a dose-dependent bell-shaped model (Fig. 2J).

Erdr1 effect in IL-1β production also correlates with cell density in macrophages

My observations above were made using samples with cell density of 0.6 × 10^6 cells/ml. Given that previous research has indicated that the effect of Erdr1 on cell viability can be influenced by cell density (1) and that cell density–dependent inhibition has also been observed to play a role in controlling the inflammation process (22, 23), I investigated whether Erdr1's function is affected by cell density and whether Erdr1 influences cell viability in macrophages.

I observed that cell density influences both the basal and LPS-induced proinflammatory responses, as well as cell viability (Supplemental Fig. 2A, 2B). Additionally, cell density affects the expression pattern and subcellular localization of Erdr1 (Supplemental Figs. 2C, 3A–B). Erdr1 typically exhibits high expression levels and tends to localize in the cytoplasm at high cell density, whereas at low cell density, it is characterized by low expression levels and nuclear localization (Supplemental Figs. 2C, 3A, 3B). Moreover, endogenous Erdr1 demonstrates a positive correlation with IL-1β at low cell density, while it manifests a negative correlation with IL-1β at high cell densities upon LPS stimulation.

I further discovered that the Erdr1 protein modulates IL-1β expression (Supplemental Fig. 2D, 2G) and cell viability (Supplemental Fig. 2E, 2H) in a manner that is distinctly influenced by cell density. Overall, Erdr1 emerges as an amplifier of the proinflammatory response under conditions of low cell density yet transitions into an inhibitor of the proinflammatory response when cell density is high.

I also discovered that Erdr1 protein can regulate the intrinsic Erdr1 expression (Supplemental Fig. 2F, 2I), which was found to correlate with cell viability (Supplemental Fig. 2E, 2H). Both downregulation and upregulation of Erdr1 are associated with decreased cell viability, suggesting that endogenous Erdr1 plays a crucial role in maintaining cellular homeostasis. It is becoming clear that controlled fluctuations in endogenous Erdr1 levels are

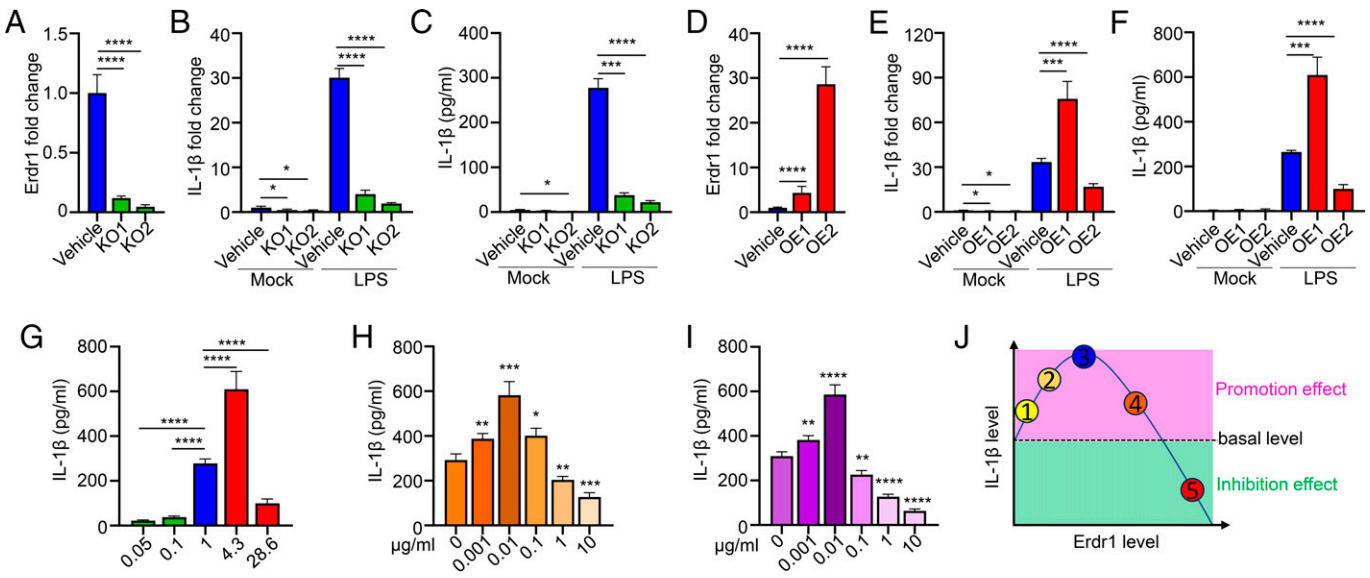

FIGURE 2. Erdr1 has a dose-dependent bell-shaped effect in LPS-induced IL-1β production in macrophages.

(**A–C**) Knockout of Erdr1 in BMDM by lentivirus transduction for 40 h and then treated without or with 1 μg/ml LPS for 24 h for the following analysis. Erdr1 KO1 and Erdr1 KO2 represent two knockout vectors. The vehicle is transfected with the control lentivirus vector ($n = 4$). (A) qPCR detecting Erdr1 expression after lentivirus transduction for 40 h. (B) qPCR detecting IL-1β expression. (C) Detecting IL-1β production at supernatant by ELISA. (**D–F**) Overexpression of Erdr1 in BMDM by lentivirus transduction for 40 h and then treated without or with 1 μg/ml LPS for 24 h for the following analysis. Erdr1 OE1 and Erdr1 OE2 represent two transfection titers of lentivirus. The vehicle is transfected with the control lentivirus vector ($n = 4$). (D) qPCR detecting Erdr1 expression after lentivirus transduction for 40 h. (E) qPCR detecting IL-1β expression. (F) Detecting IL-1β production at supernatant by ELISA. (**G**) The correlation of endogenous Erdr1 level (qPCR) and IL-1β level (ELISA) summary from (C) and (F). (**H**) Detecting IL-1β level at supernatant by ELISA in 1 μg/ml LPS-induced BMDM with the indicated concentration of Erdr1 Abs treatment ($n = 4$). (**I**) Detecting IL-1β level at supernatant by ELISA in 1 μg/ml LPS-induced BMDM with the indicated concentration of purified full-length Erdr1 protein treatment ($n = 4$). (**J**) Threshold model of Erdr1 in IL-1β production: a bell-shaped function in IL-1β production. Points 1 and 2 show that a low level of Erdr1 has a positive correlation with IL-1β. Point 3 shows that the optimal Erdr1 concentration promotes the peak expression of IL-1β. Points 4 and 5 show that a high level of Erdr1 has a negative correlation with IL-1β level. These show that Erdr1 has both positive and negative roles in IL-1β production by dose change. (A–I) Cell density is 0.6×10^6/ml and seeded in 24-well plates. All qPCR results were normalized to β-actin expression. The data represent mean ± SD. *$p < 0.05$, **$p < 0.01$, ***$p < 0.001$, ****$p < 0.0001$. The data are representative of three independent experiments.

pivotal in facilitating cellular survival, whereas deviations from these levels may promote cell death (see below). In summary, these data demonstrate that the effect of Erdr1 on the macrophage inflammatory response is closely correlated with cell density.

Erdr1 promotes IL-1β production through activating YAP1 and Mid1 signaling pathway

I further explored the mechanism of the dual role of Erdr1 in regulating IL-1β production. I hypothesized that YAP1 and Mid1 are involved in this process as previously stated.

To validate this hypothesis, I examined whether and how YAP1 and Mid1 are regulated in M1/M2 macrophages. I observed remarkable upregulation of Mid1 and YAP1 in M1 macrophages compared with M0 macrophages (Fig. 3A, 3B; Supplemental Fig. 1A). In contrast, I observed a significant decrease in the expression of Mid1 and YAP1 (Fig. 3A, 3B) in M2 macrophages. These findings indicate that Mid1 and YAP1 are distinctly regulated in M1/M2 macrophages. Utilizing immunofluorescence, I investigated the subcellular localization of YAP1 and Mid1 in M1/M2 macrophages. YAP1 has increased nuclear localization in M1 macrophages but increased cytoplasmic localization in M2 macrophages (Fig. 3C). Conversely, I observed remarkably increased cytoplasm localization of Mid1 in M1 macrophages but increased nuclear localization in M2 macrophages compared with M0 macrophages (Fig. 3D). I further validated these observations using ImageJ (Fig. 3E, 3F). These findings reveal that Mid1 and YAP1 exhibit dynamic regulation and distinct subcellular localization patterns during macrophage polarization.

I further investigated whether YAP1 and Mid1 are involved in Erdr1-mediated, LPS-induced IL-1β production. The data demonstrate that the knockout of Mid1, YAP1, or both leads to a significant blockade of IL-1β production in macrophages induced by LPS (Fig. 3G), indicating that Mid1 and YAP1 are both essential for IL-1β production in M1 macrophages. Moderate overexpression of Erdr1 (Erdr1 OE1) has been shown to

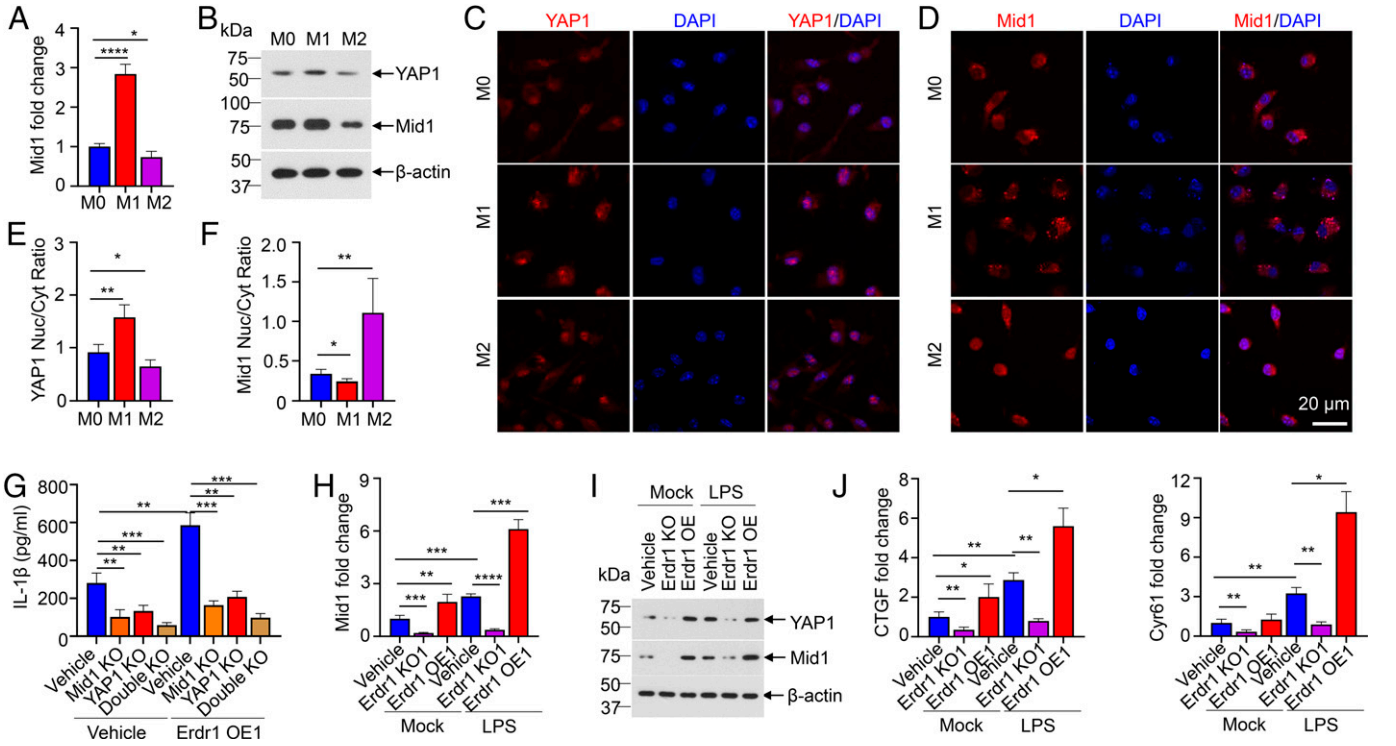

FIGURE 3. Erdr1 modulates IL-1β production through the regulation of YAP1 and Mid1 signaling pathways.

(**A**) qPCR analysis of Mid1 expression in M0, M1, and M2 macrophages ($n = 4$). (**B**) Immunoblot analysis of YAP1 and Mid1 levels in the cell lysates of M0, M1, and M2 macrophages. (**C** and **D**) Immunofluorescence staining of YAP1 (C) and Mid1 (D) in M0, M1, and M2 macrophages and counterstained by DAPI. Scale bar, 20 μm. (**E** and **F**) Nuclear to cytoplasm (Neu/Cyt) intensity ratios YAP1 (E) and Mid1 (F) were quantified by ImageJ. $n = 5$ with more than 10 macrophages were analyzed per sample. (**G**) Detecting IL-1β production by ELISA in the indicated BMDM group before and after 1 μg/ml LPS stimulation for 24 h ($n = 4$). Mid1 KO, YAP1 KO, and double KO represent knockout Mid1, YAP1, and both Mid1/YAP1 in BMDM by transfection CRISPR/cas9 lentivirus; Erdr1 OE1 represent moderate overexpression of Erdr1 (~4 folds) in BMDM by transfection lentivirus; the vehicle is transfected with the control lentivirus vector ($n = 4$). (**H–J**) BMDMs were knockout Erdr1 (Erdr1 KO1) or moderate overexpressed Erdr1 (Erdr1 OE1) and then treated without or with 1 μg/ml LPS for 24 h for following analysis. (H) qPCR analysis of Mid1 expression ($n = 4$). (I) Immunoblot analysis of YAP1 and Mid1 expression. (J) qPCR analysis of CTGF (*left*) and Cyr61 (*right*) ($n = 4$). All qPCR results were normalized to β-actin expression. (A–J) Cell density is 0.6×10^6/ml and seeded in 24-well plates. The data represent mean ± SD. *$p < 0.05$, **$p < 0.01$, ***$p < 0.001$, ****$p < 0.0001$. The data are representative of two or three independent experiments.

promote LPS-induced IL-1β production in macrophages (Fig. 2F); however, this promotive role is effectively blocked in Mid1 knockout, YAP1 knockout, or Mid1/YAP1 double knockout macrophages (Fig. 3G). These findings suggest that Erdr1 promotes IL-1β production through YAP1 and Mid1 signaling pathways.

I next tested whether Erdr1 is the upstream regulator of the YAP1 and Mid1 signaling pathways. My data show that Erdr1 overexpression (Erdr1 OE1) in macrophages, which enhances LPS-induced IL-1β production (Fig. 2F), also promotes LPS-induced Mid1 and YAP1 expression (Fig. 3H, 3I). Conversely, in Erdr1-deficient macrophages, which block IL-1β production, Mid1 and YAP1 expression is dramatically suppressed (Fig. 3H, 3I). These results indicate that Erdr1's regulation of IL-1β production is achieved by directly regulating YAP1 and Mid1 expression. Furthermore, I demonstrate that other YAP1 and Mid1 downstream genes, such as CTGF and Cyr61 (49, 57, 58), are also regulated by Erdr1 (Fig. 3J), with Erdr1 overexpression (Erdr1 OE1) promoting CTGF and Cyr61 expression, but they are inhibited in Erdr1 deficiency macrophage (Fig. 3J). This provides additional evidence that Erdr1 acts as an upstream regulator of YAP1 and Mid1. Taken together, these findings provide compelling evidence that Erdr1 plays a crucial role in promoting IL-1β production by activating YAP1 and Mid1 signaling pathways in macrophages.

Erdr1 modulates macrophage inflammatory response via dynamic interactions with YAP1 and Mid1

I hypothesized Erdr1 plays a dual role in macrophage inflammatory response by distinct interactions with YAP1 and Mid1. To investigate this, I employed coimmunoprecipitation to detect the potential interaction of Erdr1 with YAP1 and Mid1 by using 293T cells. Specifically, I hypothesized that the C-terminal domain of Erdr1 is the region responsible for interacting with YAP1. This hypothesis is grounded in previous research, which has shown that the Erdr1 C-terminal 81 amino acids are involved

in contact inhibition (2). I predicted, through analysis conducted with UniProt, that the C-terminal 32 amino acids of Erdr1 are essential for its binding to YAP1. My data manifest this by the observation that full-length Erdr1 (Erdr1–177) has direct interaction with YAP1, whereas the Erdr1 variant lacking the C-terminal 32 amino acids (Erdr1Δ32 or Erdr1–145) fails to exhibit this interaction (Fig. 4A). The direct interaction of YAP1 with Erdr1–177 but not Erdr1–145 was found in cytoplasm when coexpressed in HeLa cells (Fig. 4C). Furthermore, my data show that Mid1 has direct interaction with Erdr1–177 and an even stronger interaction with Erdr1–145 (Fig. 4B). At the same time, both Erdr1–177 and Erdr1–145 were found to interact with Mid1 at the nuclear envelope when overexpressed in HeLa cells. However, only Erdr1–145, but not Erdr1–177, demonstrates the ability to activate Mid1 and induce its translocation to the cytoplasm (Fig. 4D). These data suggest Erdr1 has the potential for distinct interactions with YAP1 and Mid1.

I predict that these distinct interactions occur because Erdr1 undergoes conformational changes at varying concentrations. By utilizing AlphaFold for protein structure prediction, I have discovered that Erdr1–177 and Erdr1–145 exhibit distinct conformations (Fig. 5B, 5C). Erdr1 contains the HESTH sequence (118–122) (Fig. 5A–C), which belongs to the zinc-binding motif HEXXH, a common feature among many zinc metalloproteinases (51) and some members of the ZIP family of zinc transporters (59). In Erdr1–177, the zinc-binding site is concealed within the loop structure (Fig. 5B), whereas in Erdr1–145, it is exposed (Fig. 5C). Using an intracellular zinc indicator, I observed an increase in intracellular free zinc induced by LPS (Fig. 5D), which is crucial for the production

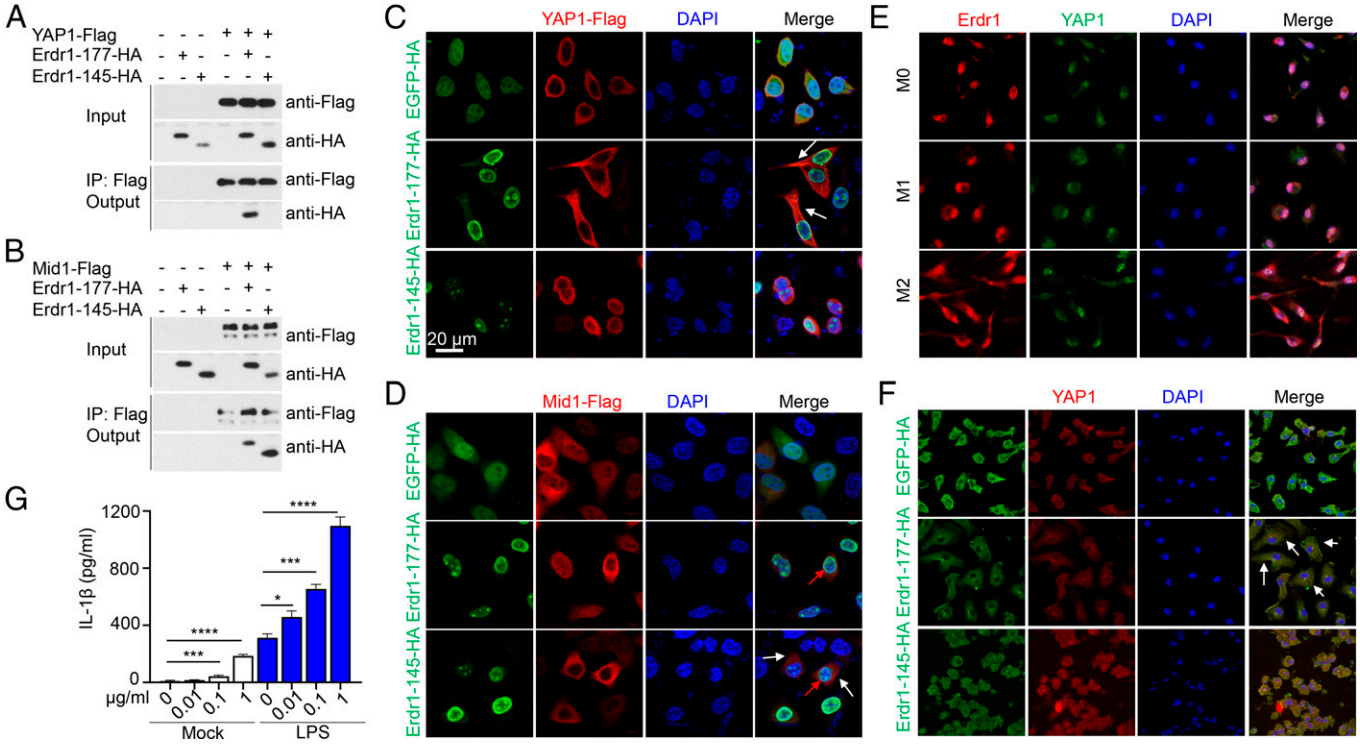

FIGURE 4. Erdr1 modulates macrophage inflammatory response via dynamic interactions with YAP1 and Mid1.

(**A** and **B**) Coimmunoprecipitation and immunoblot analysis. Flag tag proteins YAP-Flag (A) and Mid1-Flag (B) and HA tag proteins (Erdr1–177-HA and Erdr1–145-HA) were coexpressed in 293 T cells for 24 h, and cell lysates were subjected to immunoprecipitation (IP) using Flag beads. Both inputs and coimmunoprecipitation fractions (Output) were subjected to immunoblotting with anti-Flag or anti-HA Abs as indicated. Erdr1–177, full-length Erdr1; Erdr1–145, deficiency in C-terminal 32–amino acid domain. Flag tag and HA tag were added at the C terminus of the gene. (**C**) Co-overexpression of YAP1-Flag with Erdr1-177-HA or Erdr1-145-HA in Hela cell and fluorescence staining using anti-HA and anti-Flag Abs. White arrows point to the direct interaction of Erdr1-177-HA with YAP1-Flag in the cytoplasm. (**D**) Co-overexpression of Mid1-Flag with Erdr1-177-HA or Erdr1-145-HA in Hela cell and fluorescence staining using anti-HA and anti-Flag Abs. Red arrows point to the direct interaction of Mid1-Flag and Erdr1-177-HA/Erdr1-145-HA at the nuclear membrane. White arrows indicated Erdr1-145 promoted Mid1 localized at cytoplasm. (**E**) Immunofluorescence staining of endogenous Erdr1 and YAP1 in M0, M1, and M2 macrophages. (**F**) Immunofluorescence staining of overexpressed Erdr1-177-HA or Erdr1-145-HA by anti-HA Ab and endogenous YAP1 in BMDM. White arrows indicated the direct interaction of Erdr1-177 with YAP1 in the cytoplasm. Scale bar was marked in (D), it in represents 20 μm. (**G**) Detecting IL-1β production at supernatant with the indicated concentration of Erdr1-145 treatment in BMDM without or with 1 μg/ml LPS stimulation for 24 h (n = 4). The data represent mean ± SD. *$p < 0.05$, ***$p < 0.001$, ****$p < 0.001$. The data are representative of two independent experiments.

https://doi.org/10.4049/immunohorizons.2400004

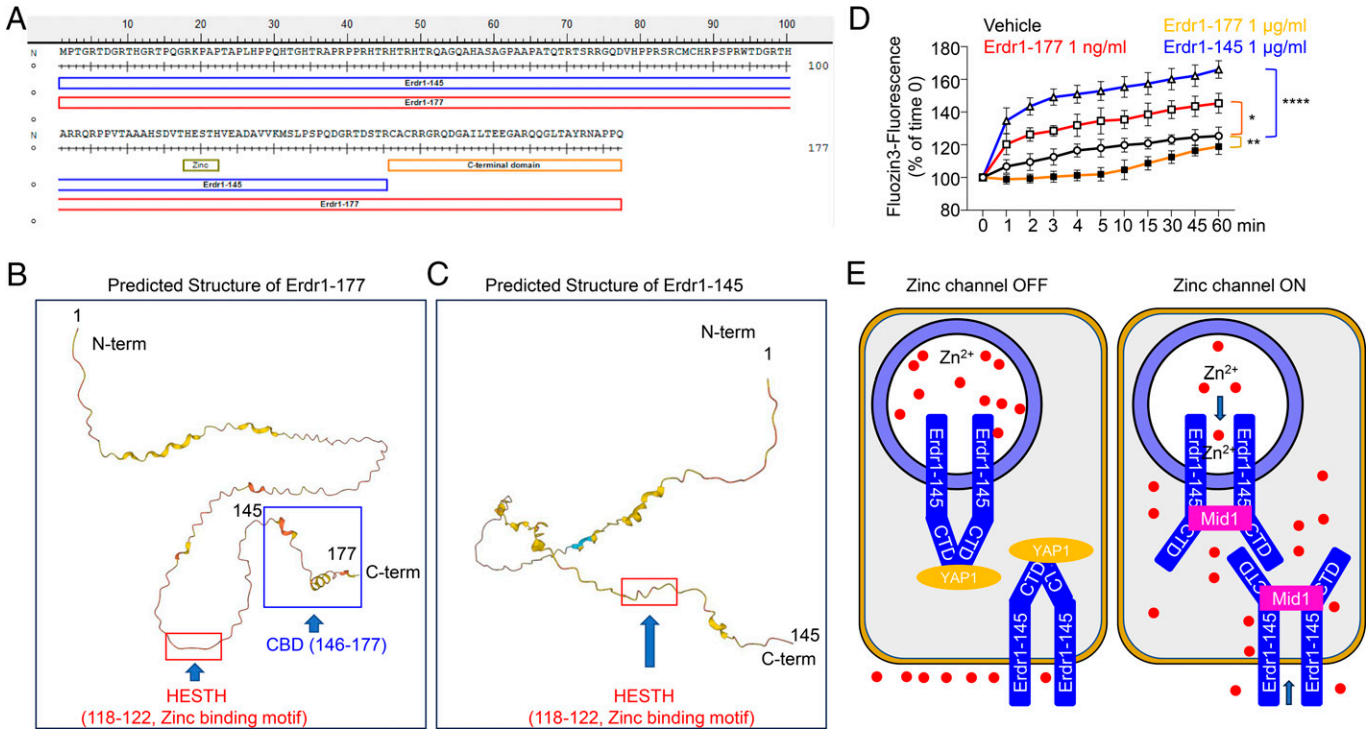

FIGURE 5. Erdr1 is a potent zinc channel by displaying different conformation.

(**A**) Full-length Erdr1 (Erdr1–177) and C-terminal 32–amino acid deficiency Erdr1 (Erdr1–145) amino acid sequence. There is a potent zinc-binding motif, HESTH (positions 118–122). The C-terminal domain indicates the YAP1 binding domain. (**B** and **C**) AlphaFold structure prediction of Erdr1–177 (https://alphafold.ebi.ac.uk/entry/O88727) (B) and Erdr1–145 (https://alphafold.ebi.ac.uk/entry/Q6PED5) (C). The potent zinc-binding motif HEXXH (positions 118–122) displayed hidden in Erdr1–177 but was exposed in Erdr1–145. (**D**) Detecting the intracellular zinc mobilization with zinc indicator. RAW-246.7 cells cultured in 96-well plates with 0.6 × 10^6 cells/ml were treated with 1 μg/ml LPS, 10 μM $ZnCl_2$, the indicated Erdr1 protein, and 1 μM FluoZin–3-acetoxymethyl ester in serum-free medium. The displayed values represent fluorescence (excitation/emission, 494/516) normalized to the initial time point (time 0). The *p* values were determined by two-way ANOVA. *$p < 0.05$, **$p < 0.01$, ****$p < 0.001$. One representative experiment of mean ± SD of $n = 4$ experiments is shown. (**E**) Working model of Erdr1 acts as a zinc channel. Zinc channel off achieved by Erdr1–YAP1 interplay. The zinc channel was achieved by Erdr1–Mid1 interplay.

of proinflammatory cytokines (60). Zinc influx can be enhanced by Erdr1–145 or low concentrations of Erdr1–177 (1 ng/ml) but can be suppressed by high concentrations of Erdr1–177 (1 μg/ml) in macrophages (Fig. 5D). These findings suggest that Erdr1's potential to interact with YAP1 and Mid1 is facilitated by conformational changes (Fig. 5E).

The endogenous Erdr1 and YAP1 interaction was robustly detected in the cytoplasm of M2 macrophages but not observed in M1 macrophages (Fig. 4E). According to my hypothesis, Erdr1 drives macrophage anti-inflammatory reprogramming through interplay with YAP1 and proinflammatory reprogramming through interaction with Mid1. Erdr1–177, which interacts with YAP1 at high concentrations, can be considered to exhibit an anti-inflammatory conformation. Conversely, Erdr1–145, which interacts with Mid1, can be considered to display a proinflammatory conformation. I further explored the impact of Erdr1–177 and Erdr1–145 on the subcellular localization of endogenous YAP1 in macrophages. BMDMs were overexpressed with Erdr1–177 or Erdr1–145 via lentivirus transduction. I observed that overexpression of Erdr1–177 leads to the sequestration of YAP1 in the cytoplasm (Fig. 4F) and induces a significant upregulation of IL-10 and TGF-β mRNA expression (Supplemental Fig. 4A), suggesting that overexpression of Erdr1–177 mediates macrophage anti-inflammatory reprogramming. However, overexpression of Erdr1–145 results in nuclear localization of YAP1 (Fig. 4F) and a significant upregulation of IL-6 and TNF expression (Supplemental Fig. 4B), indicating that Erdr1–145 overexpression drives macrophage proinflammatory reprogramming. I also employed purified Erdr1–177 and Erdr1–145 proteins to assess their roles in mediating the macrophage inflammatory response. My findings reveal that a high concentration of Erdr1–177 (1 μg/ml) spontaneously induces the expression of M2 marker genes, such as IL-10 and TGF-β (Supplemental Fig. 4C). Conversely, a high concentration of Erdr1–145 (1 μg/ml) induced the expression of IL-6 and TNF, markers for M1 macrophages (Supplemental Fig. 4D). Notably, Erdr1–145 exhibits a dose-dependent effect on priming IL-1β production and can enhance LPS-induced IL-1β production (Fig. 4G). Overall, these observations robustly reinforce my hypothesis that Erdr1 possesses the potential to function

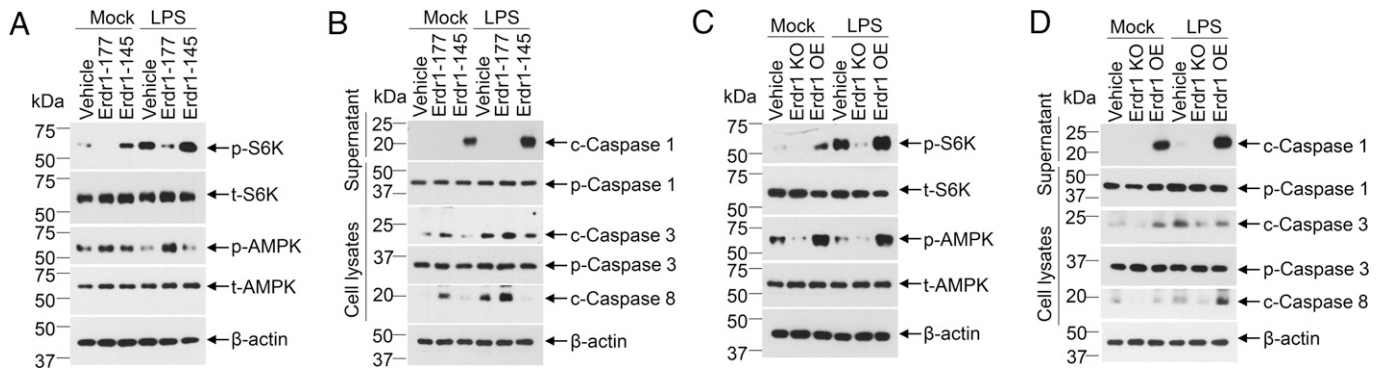

FIGURE 6. Erdr1 mediates macrophage metabolic reprogramming and determines cell death phenotypes.

(**A** and **B**) BMDMs were treated as follows for 24 h: lanes 1, vehicle; lanes 2, Erdr1–177 (1 μg/ml); lanes 3, Erdr1–145 (1 μg/ml); lanes 4, vehicle + LPS (1 μg/ml); lanes 5, Erdr1–177 (1 μg/ml) + LPS (1 μg/ml); and lanes 6, Erdr1–145 (1 μg/ml) + LPS (1 μg/ml). Cell lysates and supernatant were collected for the following analyses. (A) Immunoblot analysis of key proteins involved in metabolism as indicated. (B) Immunoblot analysis of key proteins involved in apoptosis and pyroptosis as indicated. (**C** and **D**) BMDMs were genetic knockout of Erdr1 (Erdr1 KO) or overexpressed Erdr1 (Erdr1 OE) by lentivirus transduction. The vehicle represents transduction with vehicle control lentivirus. Cell lysates were collected for immunoblot analysis with indicated Abs without and with 1 μg/ml LPS treatment for 24 h. p-S6K, phospho-S6K; t-S6K, total S6K; p-AMPK, phospho-AMPK; t-AMPK, total AMPK; p-Caspase1, pro-caspase1; c-Caspase1, cleaved caspase1; p-Caspase3, pro-caspase3; c-caspase3, cleaved caspase3; c-caspase8, cleaved caspase8. (A–D) Cell density is 0.6×10^6/ml and seeded in 24-well plates. The data represent mean ± SD. *$p < 0.05$, **$p < 0.01$, ***$p < 0.001$, ****$p < 0.0001$. The data are representative of three independent experiments.

both as an inhibitor and as an activator in the inflammatory response, facilitated by its dynamic interactions with YAP1 and Mid1.

Erdr1 drives macrophage metabolic reprogramming and determines cell fate

Reprogrammed macrophages not only exhibit distinct functions but also undergo metabolic reprogramming (61) and ultimately display varied patterns of cell death (62–64). I further explored the role of Erdr1 in the metabolic reprogramming and cell fate determination of macrophages.

Macrophage M1 polarization is characterized by the activation of mTORC1-S6K signaling (61), indicative of an anabolic state. Conversely, M2 polarization of macrophages is marked by the activation of AMPK signaling (61), reflecting a catabolic state. My findings reveal that the Erdr1–177 protein inhibits p-S6K activation while promoting p-AMPK activation in both basal and LPS-stimulated macrophages (Fig. 6A). In stark contrast, the Erdr1–145 protein significantly promotes p-S6K activation but inhibits p-AMPK activation in basal and LPS-stimulated macrophages, compared with the vehicle control (Fig. 6A). These results suggest that Erdr1 can potentially redirect macrophage reprogramming toward either a proanabolic or a procatabolic state through conformational changes. Additionally, macrophages deficient in Erdr1 show reduced basal and LPS-induced activation of both p-S6K and p-AMPK, whereas macrophages overexpressing Erdr1 exhibit enhanced activation of these pathways (Fig. 6C). This implies that Erdr1 plays a crucial role in both the anabolic and catabolic processes.

Furthermore, activated macrophages exhibit distinct cell death phenotypes. M2 macrophages undergo apoptotic death, eliciting an anti-inflammatory response. In contrast, M1 macrophages undergo pyroptosis, a proinflammatory form of cell death (62–64). My findings indicate that supplementation with either Erdr1–177 or Erdr1–145 protein promotes cell death in unstimulated macrophages (Supplemental Fig. 4E). However, Erdr1–177 protects LPS-induced macrophages from death, whereas Erdr1–145 exacerbates LPS-induced cell death (Supplemental Fig. 4E). My data further demonstrate that Erdr1–177 promotes apoptosis by enhancing the activation of caspase-3 and caspase-8, whereas it inhibits pyroptosis by reducing caspase-1 activation in macrophages (Fig. 6B). This suggests that Erdr1–177 acts as a proapoptotic factor. Conversely, Erdr1–145 inhibits apoptosis and promotes pyroptosis in both unstimulated and LPS-stimulated macrophages (Fig. 6B), supporting its potential role as a propyroptotic factor. I also observed that Erdr1 overexpression enhances the activation of both caspase-3/caspase-8 and caspase-1 in macrophages compared with the control (Fig. 6D), implying that Erdr1 is crucial for the programmed cell death process. Macrophages deficient in Erdr1 lacked caspase-dependent programmed cell death (Fig. 6D) but still showed reduced cell viability (Supplemental Fig. 4F), indicating that an optimal level of Erdr1 is essential for cell survival; otherwise, Erdr1 mediates cell death.

In summary, my findings indicate that Erdr1 mediates macrophage metabolic reprogramming and determines cell fate. Dysregulated Erdr1 levels lead to macrophage programmed cell death through either a proapoptotic or propyroptotic pathway (Fig. 7A, 7B).

https://doi.org/10.4049/immunohorizons.2400004

DISCUSSION

This study aimed to elucidate the role of Erdr1 in the bidirectional regulation of the macrophage inflammatory response. I have uncovered that Erdr1 functions through a dynamic interaction with YAP1 and Mid1. This interplay not only modulates macrophage inflammatory response but also drives metabolic reprogramming, thereby underscoring Erdr1's pivotal role in macrophage programming.

Erdr1 has been found to exhibit a negative correlation with IL-18 (55), and purified Erdr1 protein has played an anti-inflammatory role by inhibiting the production of various cytokines, such as TNF, IL-6, and IL-1β (8, 56). My data further underscore the anti-inflammatory role of Erdr1. Interestingly, I have also uncovered that Erdr1 can assume a proinflammatory role, which is closely associated with the dosage of Erdr1 and cell densities. Both extrinsic and intrinsic Erdr1 contribute to IL-1β production in a dose-dependent, bell-shaped model. This threshold model has been similarly observed in Erdr1-mediated metastasis in murine embryonic fibroblasts (29, 65), indicating that Erdr1 functions are highly dynamic. I found that Erdr1 is significantly upregulated in M2 macrophages and may serve as an M2 marker gene, aligning with previous research (66). It is worth noting that Erdr1 was found to be dramatically suppressed in M1 macrophages. Downregulation of Erdr1 has also been observed in other immune and nonimmune cells upon activation. For instance, Erdr1 showed downregulation in $CD4^+$ T cells upon TCR stimulation (5) and was also downregulated

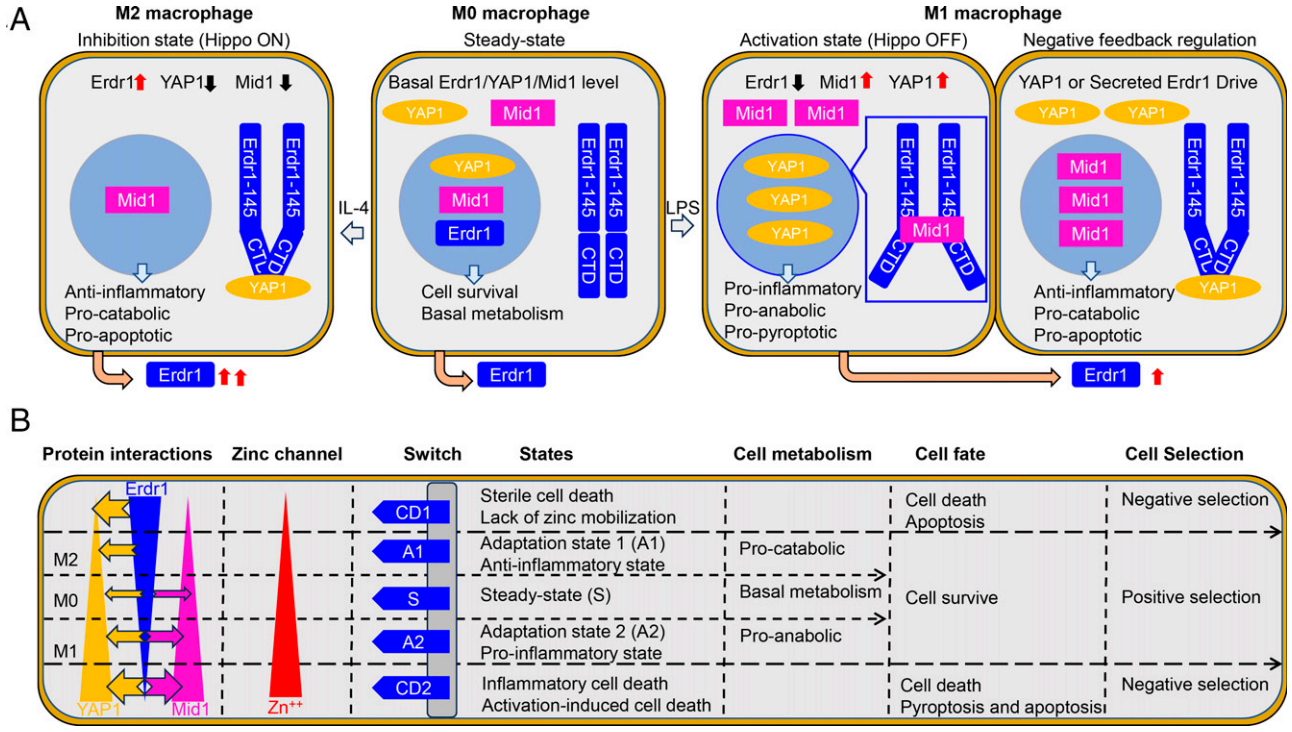

FIGURE 7. Working model of Erdr1 in macrophages reprogramming and cell fate determination.

(**A**) Erdr1 drives macrophage reprogramming. Erdr1 has concentration and conformation change during macrophage polarization and plays multifunction in M1 and M2 macrophage. The M0 macrophage represents the steady state of macrophage with basal levels of Erdr1, Mid1, and YAP1 expression, accompanied by a basal metabolism level. Erdr1 acts as a cell survival factor at this state. M0 macrophages are induced to M2 macrophages with 20 ng/ml IL-4 treatment for 24 h. In M2 macrophages, Erdr1 is endogenously upregulated, with increased cytoplasm localization and increased secretion to the extracellular matrix. The upregulated Erdr1 interacts with YAP1 through its C-terminal domain (Erdr1-CBD), which consists of 32 amino acids. This interaction sequesters YAP1 in the cytoplasm and reduces YAP1 expression (Hippo ON), consequently leading to Mid1 inactivation. Erdr1 acts as an anti-inflammatory, procatabolic, and proapoptotic factor in M2 state. M1 macrophages are induced from M0 macrophages by 1 μg/ml LPS treatment for 24 h. In M1 macrophages, Erdr1 is endogenously downregulated and increased nuclear localization but increased release to extracellular matrix. The downregulated Erdr1 undergoes conformation shift and exhibits a high affinity with Mid1 through its Erdr1–145 domain (Erdr1–145, or Erdr1Δ32) at the nuclear envelope and forces YAP1 ON. Erdr1 acts as a proinflammatory, proanabolic and propyroptotic factor in M1 state. Additionally, negative feedback regulation can be initiated in M1 macrophage by upregulated endogenous YAP1 and increased accumulation of secreted Erdr1. This figure illustrates the main expression level (red arrows indicate upregulated, and black arrows indicate downregulated), subcellular localization, and dynamic interaction of Erdr1 with Mid1and YAP1 in M0, M1, and M2 macrophages. (**B**) Working model of Erdr1 in cell fate determination. The interplay of Erdr1 with Mid1 and YAP1 shapes macrophage heterogeneity and determines the cell survival or death and the death patterns. CTD, C-terminal domain.

in tissues from patients with inflammatory disorders (9, 10, 56), in tumor cells (55), and in bleomycin-induced fibroblasts (50). This suggests that decreased Erdr1 levels act to activate specific cellular functions. My data indicate that reduced Erdr1 undergoes a conformational change and promotes a proinflammatory response through interaction with Mid1, whereas elevated Erdr1 enhances the anti-inflammatory response through interaction with YAP1.

YAP1 has been shown to mediate macrophage polarization and enhance proinflammatory cytokine production in macrophages (67–69). Mid1 is also involved in macrophage activation (23–25). In line with previous studies (49, 67, 69), I observed a significant upregulation of YAP1 and Mid1 expression in proinflammatory macrophages. Importantly, both YAP1 and Mid1 are crucial for the Erdr1-mediated LPS-induced production of IL-1β. I have discovered that Erdr1 acts as an upstream regulator of YAP1 and Mid1, influencing their expression, subcellular localization, and downstream gene expression, including that of IL-1β. Furthermore, YAP1 and Mid1 have been implicated as promoters of fibrosis (49, 57). A decrease in Erdr1 expression has been linked to the pathogenesis of bleomycin-induced fibrosis in fibroblasts (50). CTGF, a central mediator of fibrosis (70) and a hallmark gene of YAP1 and Mid1 signaling (49, 58), is significantly influenced by Erdr1 (Fig. 3J). This suggests that Erdr1's regulation of YAP1 and Mid1 extends to the modulation of fibrosis pathogenesis.

Metabolic programming is a crucial hallmark of macrophage polarization. Both YAP1 and Mid1 have been shown to promote a proanabolic response (18, 71–74). Notably, Erdr1's involvement in YAP1 and Mid1-mediated metabolism has been documented (18, 32). YAP1 is essential for mTOR signaling; its deficiency in dental epithelial stem cells leads to reduced Erdr1 expression, subsequently inhibiting mTOR signaling (18). Furthermore, increased levels of Erdr1 and Mid1 have been associated with a distinct metabolic profile in β-cells with the SLC30A8 (zinc transporter) R138X mutation (32). Mid1 has been identified as a key regulator of mTORC1–p-S6K signaling (71–73). These findings suggest that Erdr1 may augment mTOR signaling through interactions with YAP1 and Mid1. This aligns with my observations that Erdr1 can activate YAP1 and Mid1 signaling, thereby promoting a proanabolic state through p-S6K activation. However, my data also reveal that Erdr1 possesses a procatabolic potential by activating p-AMPK at high concentrations, a phenomenon previously observed in T cells at elevated Erdr1 levels (75). To my knowledge, my experiments involving Erdr1 knockout and overexpression (Fig. 6C) demonstrate for the first time that Erdr1 is vital for both anabolic and catabolic processes. Interestingly, the two distinct conformations of Erdr1 can mediate metabolic reprogramming toward either a procatabolic or proanabolic state, yet they antagonize each other (Fig. 6A). This suggests that Erdr1, by binding to YAP1 and Mid1 with varying affinities, directs metabolic programming toward different states. Given that p-AMPK activation is associated with M2 macrophage polarization (76) and that mTOR-p-S6K activation is linked to IL-1β production in M1 macrophages (77), my findings further underscore the role of Erdr1 in modulating the macrophage inflammatory response through metabolic reprogramming.

YAP1 has been identified as a critical regulator of cell death phenotypes (78, 79). When activated, YAP1 inhibits apoptosis (78, 79) but promotes inflammatory activation and pyroptosis in macrophages (68). In contrast, the ablation of YAP1 leads to enhanced caspase-3/8/9–dependent cell death (80). Consistent with previous findings that Erdr1 acts as a proapoptotic factor by inducing caspase-3 activation (5, 81), my data corroborate this and reveal that Erdr1, by inhibiting YAP1, triggers the activation of caspase-3 and caspase-8, thereby promoting apoptosis (Fig. 6B, 6D). Erdr1 is also linked to caspase-1 and has been implicated in the progression of degenerative diseases (82). My findings elucidate the propyroptotic role of Erdr1 (Fig. 6B, 6D) by activating YAP1. I also observed that Erdr1 mediates cell survival within a narrow range; beyond this, it precipitates rapid cell death (65). This observation aligns with Erdr1's critical involvement in cellular metabolic processes. My data demonstrate that Erdr1 is pivotal for programmed cell death and cell fate determination through the following: 1) The Erdr1–YAP1 interaction, which induces a proapoptotic response; and 2) the Erdr1–Mid1 interaction, which initiates propyroptotic activation. Additionally, negative feedback mechanisms exist that involve increased YAP1 activity or elevated extracellular accumulation of Erdr1, enhancing the Erdr1–YAP1 interaction and subsequently promoting apoptotic cell death, which serves to mitigate inflammation.

YAP1 serves as a downstream effector of the Hippo pathway, a highly conserved signaling pathway that governs organ size by regulating cell proliferation, apoptosis, and stem cell self-renewal (83). The function of YAP1 is intricately linked to its expression levels and subcellular localization. YAP1 is inactivated (and the Hippo pathway activated) when sequestered in the cytoplasm, leading to the inhibition of YAP1 signaling (83). Extensive research over the years has shown that Hippo pathway activation can be achieved through a sequential cascade of kinase activations, including LATS1/2 kinases (83). However, a distinct mechanism of YAP1 regulation, independent of LATS1/2 kinases, has been observed in Tregs cells, which exhibit altered levels of Erdr1 and Mid1(19). Mechanical cues, including cell density, have consistently been shown to regulate Hippo-YAP signaling by mediating actin rearrangement (17, 68, 84–86). Erdr1 is implicated in actin modulation (6) and exhibits cell density-dependent functions. It is highly plausible that Erdr1 acts as a sensor, working in concert with Mid1 to convert mechanical cues into intracellular signals, thereby facilitating actin remodeling and playing a key role in regulating the Hippo-YAP1 signaling pathway. My research suggests that factors affecting the intrinsic fluctuations of Erdr1 can modulate the Hippo-YAP1 signaling pathway. Most importantly, Erdr1 regulates YAP1 on/off through a nonclassical pathway.

However, the research progress of Erdr1 was hindered by several obstacles. Firstly, Erdr1 global knockout resulted in 100%

https://doi.org/10.4049/immunohorizons.2400004

embryonic lethality (5, 87), which limited research in mice. This also indicates that Erdr1 plays a crucial role in cell physiological processes. Secondly, although Erdr1 has been mapped to sex chromosomes in mice, it has a high GC content (65) and contains many repeats (26), making identifying the entire genome sequence of Erdr1 impossible until recently (27). Thirdly, despite human Erdr1 mRNA and protein sequences being identified as 100% identical to those of mouse Erdr1 (2, 65), a rarity in cross-species comparisons, there remains a notable absence of accessible human Erdr1 mRNA and protein data in the NCBI database. This gap is due to incomplete sequencing of the Erdr1 locus in humans (88). Consequently, this limitation obstructs the recognition of Erdr1 as a critical target for further research in human studies. There is an urgent need to map the localization of Erdr1 in the human genome and complete the gene sequencing. At the same time, it is believed that Erdr1 should also exist and be highly conserved in other species. Efforts to further explore Erdr1 across different species will contribute to a better understanding of the evolutionary process of life.

In this study, at the cellular level, I have demonstrated that Erdr1 plays a crucial role in driving macrophage functional and metabolic programming, ultimately determining cell fate through a dynamic interplay with YAP1 and Mid1 (Fig. 7A, 7B). The function of Erdr1 is dependent on the pattern, strength, and duration of extracellular stimuli. My working model suggests that Erdr1 is involved in both the positive and negative selection within the macrophage repertoire (Fig. 7B). Understanding the molecular mechanism of macrophage polarization driven by Erdr1 stands to profoundly enhance our ability to therapeutically modulate inflammation more precisely and efficiently. Moreover, it is crucial to highlight my significant observation that Erdr1 regulates YAP1 signaling through the nonclassical Hippo pathway. These findings imply the critical role of Erdr1 in maintaining cellular and tissue homeostasis, extending beyond its impact on macrophages alone. Erdr1 (5), YAP1 (89), and Mid1 (73) have also been demonstrated to be distinctly induced during T cell polarization. The negative correlation between Erdr1 and YAP1/Mid1 in activated T cells suggests that the working model of Erdr1 with YAP1 and Mid1 may also be involved in the T cell activation and selection process.

Practically, Erdr1 acts as the metabolic reprogramming factor and cell fate determiner, and the dysregulated Erdr1 might be the root cause of metabolic shifts and cell fate alters in macrophages. By modulating Erdr1, we can easily regulate the immune response of macrophages. This presents a potentially straightforward approach to addressing autoimmune disorders and immune dysregulation in infectious diseases, such as COVID-19 (90, 91).

DISCLOSURES

The author has no financial conflicts of interest.

ACKNOWLEDGMENTS

I sincerely thank Dr. Stanley Perlman from the University of Iowa for his significant contribution to the manuscript revision. My sincere appreciation also goes to Dr. Ning Li from Beijing Capital Agribusiness Co. for actively participating in the discussion and for contributing to the manuscript revision. I kindly thank my son, K.W.P., for his companionship and contributions to the ideas.

REFERENCES

1. Dörmer, P., E. Spitzer, and W. Möller. 2004. EDR is a stress-related survival factor from stroma and other tissues acting on early haematopoietic progenitors (E-Mix). *Cytokine* 27: 47–57.
2. Dörmer, P., E. Spitzer, M. Frankenberger, and E. Kremmer. 2004. Erythroid differentiation regulator (EDR), a novel, highly conserved factor I. Induction of haemoglobin synthesis in erythroleukaemic cells. *Cytokine* 26: 231–242.
3. Kim, M. S., S. Lee, S. J. Jung, S. Park, K. E. Kim, T. S. Kim, H. J. Park, and D. Cho. 2019. Erythroid differentiation regulator 1 strengthens TCR signaling in thymocytes by modulating calcium flux. *Cell. Immunol.* 336: 28–33.
4. Kim, M. S., D. Park, S. Lee, S. Park, K. E. Kim, T. S. Kim, H. J. Park, and D. Cho. 2022. Erythroid differentiation regulator 1 strengthens TCR signaling by enhancing PLCgamma1 signal transduction pathway. *Int. J. Mol. Sci.* 23: 844.
5. Soto, R., C. Petersen, C. L. Novis, J. L. Kubinak, R. Bell, W. Z. Stephens, T. E. Lane, R. S. Fujinami, A. Bosque, R. M. O'Connell, and J. L. Round. 2017. Microbiota promotes systemic T-cell survival through suppression of an apoptotic factor. *Proc. Natl. Acad. Sci. USA* 114: 5497–5502.
6. Lee, H. R., S. Y. Huh, D. Y. Hur, H. Jeong, T. S. Kim, S. Y. Kim, S. B. Park, Y. Yang, S. I. Bang, H. Park, and D. Cho. 2014. ERDR1 enhances human NK cell cytotoxicity through an actin-regulated degranulation-dependent pathway. *Cell. Immunol.* 292: 78–84.
7. Kim, M. S., S. Lee, S. Park, K. E. Kim, H. J. Park, and D. Cho. 2020. Erythroid differentiation regulator 1 ameliorates collagen-induced arthritis via activation of regulatory T cells. *Int. J. Mol. Sci.* 21: 9555.
8. Kim, K. E., S. Kim, S. Park, Y. Houh, Y. Yang, S. B. Park, S. Kim, D. Kim, D. Y. Hur, S. Kim, et al. 2016. Therapeutic effect of erythroid differentiation regulator 1 (Erdr1) on collagen-induced arthritis in DBA/1J mouse. *Oncotarget* 7: 76354–76361.
9. Kim, M., K. E. Kim, H. Y. Jung, H. Jo, S. W. Jeong, J. Lee, C. H. Kim, H. Kim, D. Cho, and H. J. Park. 2015. Recombinant erythroid differentiation regulator 1 inhibits both inflammation and angiogenesis in a mouse model of rosacea. *Exp. Dermatol.* 24: 680–685.
10. Kim, K. E., Y. Houh, J. Lee, S. Kim, D. Cho, and H. J. Park. 2016. Downregulation of erythroid differentiation regulator 1 (Erdr1) plays a critical role in psoriasis pathogenesis. *Exp. Dermatol.* 25: 570–572.
11. Zheng, D., T. Liwinski, and E. Elinav. 2020. Inflammasome activation and regulation: toward a better understanding of complex mechanisms. *Cell Discov.* 6: 36.
12. Kelley, N., D. Jeltema, Y. Duan, and Y. He. 2019. The NLRP3 inflammasome: an overview of mechanisms of activation and regulation. *Int. J. Mol. Sci.* 20: 3328.
13. Abo, H., B. Chassaing, A. Harusato, M. Quiros, J. C. Brazil, V. L. Ngo, E. Viennois, D. Merlin, A. T. Gewirtz, A. Nusrat, and T. L. Denning. 2020. Erythroid differentiation regulator-1 induced by microbiota in early life drives intestinal stem cell proliferation and regeneration. *Nat. Commun.* 11: 513.
14. Wu, J. M. F., Y. Y. Cheng, T. W. H. Tang, C. Shih, J. H. Chen, and P. C. H. Hsieh. 2018. Prostaglandin E_2 receptor 2 modulates macrophage activity for cardiac repair. *J. Am. Heart. Assoc.* 7: e009216.
15. Gumbiner, B. M., and N. G. Kim. 2014. The Hippo-YAP signaling pathway and contact inhibition of growth. *J. Cell Sci.* 127: 709–717.

16. Pavel, M., M. Renna, S. J. Park, F. M. Menzies, T. Ricketts, J. Füllgrabe, A. Ashkenazi, R. A. Frake, A. C. Lombarte, C. F. Bento, et al. 2018. Contact inhibition controls cell survival and proliferation via YAP/TAZ–autophagy axis. *Nat. Commun.* 9: 2961.
17. Zhao, B., X. Wei, W. Li, R. S. Udan, Q. Yang, J. Kim, J. Xie, T. Ikenoue, J. Yu, L. Li, et al. 2007. Inactivation of YAP oncoprotein by the Hippo pathway is involved in cell contact inhibition and tissue growth control. *Genes Dev.* 21: 2747–2761.
18. Hu, J. K., W. Du, S. J. Shelton, M. C. Oldham, C. M. DiPersio, and O. D. Klein. 2017. An FAK-YAP-mTOR signaling axis regulates stem cell-based tissue renewal in mice. *Cell Stem Cell* 21: 91–106.e6.
19. Ni, X., J. Tao, J. Barbi, Q. Chen, B. V. Park, Z. Li, N. Zhang, A. Lebid, A. Ramaswamy, P. Wei, et al. 2018. YAP is essential for Treg-mediated suppression of antitumor immunity. *Cancer Discov.* 8: 1026–1043.
20. Hamon, A., D. García-García, D. Ail, J. Bitard, A. Chesneau, D. Dalkara, M. Locker, J. E. Roger, and M. Perron. 2019. Linking YAP to Müller glia quiescence exit in the degenerative retina. *Cell Rep.* 27: 1712–1725.e6.
21. Gong, S., G. Cao, F. Li, Z. Chen, X. Pan, H. Ma, Y. Zhang, B. Yu, and J. Kou. 2021. Endothelial conditional knockdown of NMMHC IIA (nonmuscle myosin heavy chain IIA) attenuates blood–brain barrier damage during ischemia–reperfusion injury. *Stroke* 52: 1053–1064.
22. Lu, T., R. Chen, T. C. Cox, R. X. Moldrich, N. Kurniawan, G. Tan, J. K. Perry, A. Ashworth, P. F. Bartlett, L. Xu, et al. 2013. X-linked microtubule-associated protein, Mid1, regulates axon development. *Proc. Natl. Acad. Sci. USA* 110: 19131–19136.
23. Collison, A. M., J. Li, A. P. de Siqueira, X. Lv, H. D. Toop, J. C. Morris, M. R. Starkey, P. M. Hansbro, J. Zhang, and J. Mattes. 2019. TRAIL signals through the ubiquitin ligase MID1 to promote pulmonary fibrosis. *BMC Pulm. Med.* 19: 31.
24. Chen, X., L. Wang, H. Yu, Q. Shen, Y. Hou, Y. X. Xia, L. Li, L. Chang, and W. H. Li. 2023. Irradiated lung cancer cell-derived exosomes modulate macrophage polarization by inhibiting MID1 via miR-4655-5p. *Mol. Immunol.* 155: 58–68.
25. Fang, M., A. Zhang, Y. Du, W. Lu, J. Wang, L. J. Minze, T. C. Cox, X. C. Li, J. Xing, and Z. Zhang. 2022. TRIM18 is a critical regulator of viral myocarditis and organ inflammation. *J. Biomed. Sci.* 29: 55.
26. Chu, H. P., J. E. Froberg, B. Kesner, H. J. Oh, F. Ji, R. Sadreyev, S. F. Pinter, and J. T. Lee. 2017. PAR-TERRA directs homologous sex chromosome pairing. *Nat. Struct. Mol. Biol.* 24: 620–631.
27. Kasahara, T., K. Mekada, K. Abe, A. Ashworth, and T. Kato. 2022. Complete sequencing of the mouse pseudoautosomal region, the most rapidly evolving "chromosome." bioRxiv 485930.
28. Armoskus, C., D. Moreira, K. Bollinger, O. Jimenez, S. Taniguchi, and H. W. Tsai. 2014. Identification of sexually dimorphic genes in the neonatal mouse cortex and hippocampus. *Brain Res.* 1562: 23–38.
29. Mango, R. L., Q. P. Wu, M. West, E. C. McCook, J. S. Serody, and H. W. van Deventer. 2014. C-C chemokine receptor 5 on pulmonary mesenchymal cells promotes experimental metastasis via the induction of erythroid differentiation regulator 1. *Mol. Cancer Res.* 12: 274–282.
30. Kovačić, N. L. N. 2019. Mid1 is a novel mediator of subchondral bone resorption in antigen-induced arthritis. In *Fourth Annual Meeting of the European Calcified Tissue Society*, May 11–14, Budapest, Hungary.
31. Perez, E. C., P. Xander, M. F. L. Laurindo, E. B. R. R. Novaes, B. C. Vivanco, R. A. Mortara, M. Mariano, J. D. Lopes, and A. C. Keller. 2017. The axis IL-10/claudin-10 is implicated in the modulation of aggressiveness of melanoma cells by B-1 lymphocytes. *PLoS One* 12: e0187333.
32. Kleiner, S., D. Gomez, B. Megra, E. Na, R. Bhavsar, K. Cavino, Y. Xin, J. Rojas, G. Dominguez-Gutierrez, B. Zambrowicz, et al. 2018. Mice harboring the human SLC30A8 R138X loss-of-function mutation have increased insulin secretory capacity. *Proc. Natl. Acad. Sci. USA* 115: E7642–E7649.
33. Verhagen, A. M., C. A. de Graaf, T. M. Baldwin, A. Goradia, J. E. Collinge, B. T. Kile, D. Metcalf, R. Starr, and D. J. Hilton. 2012. Reduced lymphocyte longevity and homeostatic proliferation in lamin B receptor-deficient mice results in profound and progressive lymphopenia. *J. Immunol.* 188: 122–134.
34. Sferruzzi-Perri, A. N., A. M. Macpherson, C. T. Roberts, and S. A. Robertson. 2009. Csf2 null mutation alters placental gene expression and trophoblast glycogen cell and giant cell abundance in mice. *Biol. Reprod.* 81: 207–221.
35. Laufer, B. I., K. Neier, A. E. Valenzuela, D. H. Yasui, R. J. Schmidt, P. J. Lein, and J. M. LaSalle. 2022. Placenta and fetal brain share a neurodevelopmental disorder DNA methylation profile in a mouse model of prenatal PCB exposure. *Cell Rep.* 38: 110442.
36. Ratliff, W. A., D. Qubty, V. Delic, C. G. Pick, and B. A. Citron. 2020. Repetitive mild traumatic brain injury and transcription factor modulation. *J. Neurotrauma* 37: 1910–1917.
37. Jackson, I. L., F. Baye, C. P. Goswami, B. P. Katz, A. Zodda, R. Pavlovic, G. Gurung, D. Winans, and Z. Vujaskovic. 2017. Gene expression profiles among murine strains segregate with distinct differences in the progression of radiation-induced lung disease. *Dis. Model. Mech.* 10: 425–437.
38. Descalzi, G., V. Mitsi, I. Purushothaman, S. Gaspari, K. Avrampou, Y. E. Loh, L. Shen, and V. Zachariou. 2017. Neuropathic pain promotes adaptive changes in gene expression in brain networks involved in stress and depression. *Sci. Signal.* 10: eaaj1549.
39. Zhao, Z., T. Miki, A. Van Oort-Jansen, T. Matsumoto, D. S. Loose, and C. C. Lee. 2011. Hepatic gene expression profiling of 5'-AMP-induced hypometabolism in mice. *Physiol. Genomics* 43: 325–345.
40. Hou, Y. J., R. Banerjee, B. Thomas, C. Nathan, A. García-Sastre, A. Ding, and M. B. Uccellini. 2013. SARM is required for neuronal injury and cytokine production in response to central nervous system viral infection. *J. Immunol.* 191: 875–883.
41. Qiao, X., J. Y. Lu, and S. L. Hofmann. 2007. Gene expression profiling in a mouse model of infantile neuronal ceroid lipofuscinosis reveals upregulation of immediate early genes and mediators of the inflammatory response. *BMC Neurosci.* 8: 95.
42. Vijay, R., A. R. Fehr, A. M. Janowski, J. Athmer, D. L. Wheeler, M. Grunewald, R. Sompallae, S. P. Kurup, D. K. Meyerholz, F. S. Sutterwala, et al. 2017. Virus-induced inflammasome activation is suppressed by prostaglandin D_2/DP1 signaling. *Proc. Natl. Acad. Sci. USA* 114: E5444–E5453.
43. Li, W., M. J. Hofer, P. Songkhunawej, S. R. Jung, D. Hancock, G. Denyer, and I. L. Campbell. 2017. Type I interferon-regulated gene expression and signaling in murine mixed glial cells lacking signal transducers and activators of transcription 1 or 2 or interferon regulatory factor 9. *J. Biol. Chem.* 292: 5845–5859.
44. Karlsen, T. R., M. B. Olsen, X. Y. Kong, K. Yang, A. Quiles-Jiménez, P. Kroustallaki, S. Holm, G. T. Lines, P. Aukrust, T. Skarpengland, et al. 2022. NEIL3-deficient bone marrow displays decreased hematopoietic capacity and reduced telomere length. *Biochem. Biophys. Rep.* 29: 101211.
45. Rubin, C. M., D. A. van der List, J. M. Ballesteros, A. V. Goloshchapov, L. M. Chalupa, and B. Chapman. 2011. Mouse mutants for the nicotinic acetylcholine receptor β2 subunit display changes in cell adhesion and neurodegeneration response genes. *PLoS One* 6: e18626.
46. Gangaplara, A., C. Martens, E. Dahlstrom, A. Metidji, A. S. Gokhale, D. D. Glass, M. Lopez-Ocasio, R. Baur, K. Kanakabandi, S. F. Porcella, and E. M. Shevach. 2018. Type I interferon signaling attenuates regulatory T cell function in viral infection and in the tumor microenvironment. *PLoS Pathog.* 14: e1006985.
47. Pagliari, S., V. Vinarsky, F. Martino, A. R. Perestrelo, J. Oliver De La Cruz, G. Caluori, J. Vrbsky, P. Mozetic, A. Pompeiano, A. Zancla, et al. 2021. YAP-TEAD1 control of cytoskeleton dynamics and intracellular tension guides human pluripotent stem cell mesoderm specification. *Cell Death Differ.* 28: 1193–1207.

48. Mohseni, M., J. Sun, A. Lau, S. Curtis, J. Goldsmith, V. L. Fox, C. Wei, M. Frazier, O. Samson, K. K. Wong, et al. 2014. A genetic screen identifies an LKB1-MARK signalling axis controlling the Hippo-YAP pathway. *Nat. Cell Biol.* 16: 108–117.
49. Chen, Q., C. Gao, M. Wang, X. Fei, and N. Zhao. 2021. TRIM18-regulated STAT3 signaling pathway via PTP1B promotes renal epithelial–mesenchymal transition, inflammation, and fibrosis in diabetic kidney disease. *Front. Physiol.* 12: 709506.
50. Wang, Y., L. Zhang, T. Huang, G. R. Wu, Q. Zhou, F. X. Wang, L. M. Chen, F. Sun, Y. Lv, F. Xiong, et al. 2022. The methyl-CpG-binding domain 2 facilitates pulmonary fibrosis by orchestrating fibroblast to myofibroblast differentiation. *Eur. Respir. J.* 60: 2003697.
51. Fukasawa, K. M., T. Hata, Y. Ono, and J. Hirose. 2011. Metal preferences of zinc-binding motif on metalloproteases. *J. Amino Acids* 2011: 574816.
52. Wright, P. E., and H. J. Dyson. 2015. Intrinsically disordered proteins in cellular signalling and regulation. *Nat. Rev. Mol. Cell Biol.* 16: 18–29.
53. Orecchioni, M., Y. Ghosheh, A. B. Pramod, and K. Ley. 2019. Macrophage polarization: different gene signatures in M1(LPS+) vs. classically and M2(LPS−) vs. alternatively activated macrophages. *Front. Immunol.* 10: 1084.
54. Murray, P. J. 2017. Macrophage polarization. *Annu. Rev. Physiol.* 79: 541–566.
55. Jung, M. K., Y. Park, S. B. Song, S. Y. Cheon, S. Park, Y. Houh, S. Ha, H. J. Kim, J. M. Park, T. S. Kim, et al. 2011. Erythroid differentiation regulator 1, an interleukin 18-regulated gene, acts as a metastasis suppressor in melanoma. *J. Invest. Dermatol.* 131: 2096–2104.
56. Houh, Y. K., K. E. Kim, H. J. Park, and D. Cho. 2016. Roles of erythroid differentiation regulator 1 (Erdr1) on inflammatory skin diseases. *Int. J. Mol. Sci.* 17: 2059.
57. Liu, F., D. Lagares, K. M. Choi, L. Stopfer, A. Marinković, V. Vrbanac, C. K. Probst, S. E. Hiemer, T. H. Sisson, J. C. Horowitz, et al. 2015. Mechanosignaling through YAP and TAZ drives fibroblast activation and fibrosis. *Am. J. Physiol. Lung Cell. Mol. Physiol.* 308: L344–L357.
58. Shome, D., T. von Woedtke, K. Riedel, and K. Masur. 2020. The HIPPO transducer YAP and its targets CTGF and Cyr61 drive a paracrine signalling in cold atmospheric plasma-mediated wound healing. *Oxid. Med. Cell. Longev.* 2020: 4910280.
59. Bin, B. H., J. Seo, and S. T. Kim. 2018. Function, structure, and transport aspects of ZIP and ZnT zinc transporters in immune cells. *J. Immunol. Res.* 2018: 9365747.
60. Haase, H., J. L. Ober-Blöbaum, G. Engelhardt, S. Hebel, A. Heit, H. Heine, and L. Rink. 2008. Zinc signals are essential for lipopolysaccharide-induced signal transduction in monocytes. *J. Immunol.* 181: 6491–6502.
61. Kelly, B., and L. A. O'Neill. 2015. Metabolic reprogramming in macrophages and dendritic cells in innate immunity. *Cell Res.* 25: 771–784.
62. Cong, Y., Y. Wang, T. Yuan, Z. Zhang, J. Ge, Q. Meng, Z. Li, and S. Sun. 2023. Macrophages in aseptic loosening: characteristics, functions, and mechanisms. *Front. Immunol.* 14: 1122057.
63. Kloditz, K., and B. Fadeel. 2019. Three cell deaths and a funeral: macrophage clearance of cells undergoing distinct modes of cell death. *Cell Death Discov.* 5: 65.
64. Robinson, N., R. Ganesan, C. Hegedűs, K. Kovács, T. A. Kufer, and L. Virág. 2019. Programmed necrotic cell death of macrophages: Focus on pyroptosis, necroptosis, and parthanatos. *Redox Biol.* 26: 101239.
65. Mango, R. L. 2010. *Stromal promotion of metastasis by erythroid differentiation regulator 1.* Doctoral dissertation, University of North Carolina at Chapel Hill, Chapel Hill, NC.
66. Lee, D. C., C. R. Ruiz, L. Lebson, M. L. Selenica, J. Rizer, J. B. Hunt, Jr., R. Rojiani, P. Reid, S. Kammath, K. Nash, et al. 2013. Aging enhances classical activation but mitigates alternative activation in the central nervous system. *Neurobiol. Aging* 34: 1610–1620.
67. Zhou, X., W. Li, S. Wang, P. Zhang, Q. Wang, J. Xiao, C. Zhang, X. Zheng, X. Xu, S. Xue, et al. 2019. YAP aggravates inflammatory bowel disease by regulating M1/M2 macrophage polarization and gut microbial homeostasis. *Cell Rep.* 27: 1176–1189.e5.
68. Meli, V. S., H. Atcha, P. K. Veerasubramanian, R. R. Nagalla, T. U. Luu, E. Y. Chen, C. F. Guerrero-Juarez, K. Yamaga, W. Pandori, J. Y. Hsieh, et al. 2020. YAP-mediated mechanotransduction tunes the macrophage inflammatory response. *Sci. Adv.* 6: eabb8471.
69. Mia, M. M., D. M. Cibi, S. A. B. Abdul Ghani, W. Song, N. Tee, S. Ghosh, J. Mao, E. N. Olson, and M. K. Singh. 2020. YAP/TAZ deficiency reprograms macrophage phenotype and improves infarct healing and cardiac function after myocardial infarction. *PLoS Biol.* 18: e3000941.
70. Lipson, K. E., C. Wong, Y. Teng, and S. Spong. 2012. CTGF is a central mediator of tissue remodeling and fibrosis and its inhibition can reverse the process of fibrosis. *Fibrogenesis Tissue Repair* 5: S24.
71. Liu, E., C. A. Knutzen, S. Krauss, S. Schweiger, and G. G. Chiang. 2011. Control of mTORC1 signaling by the Opitz syndrome protein MID1. *Proc. Natl. Acad. Sci. USA* 108: 8680–8685.
72. Posey, K. L., F. Coustry, A. C. Veerisetty, M. G. Hossain, M. J. Gambello, and J. T. Hecht. 2019. Novel mTORC1 mechanism suggests therapeutic targets for COMPopathies. *Am. J. Pathol.* 189: 132–146.
73. Boding, L., A. K. Hansen, G. Meroni, B. B. Johansen, T. H. Braunstein, C. M. Bonefeld, M. Kongsbak, B. A. Jensen, A. Woetmann, A. R. Thomsen, et al. 2014. Midline 1 directs lytic granule exocytosis and cytotoxicity of mouse killer T cells. *Eur. J. Immunol.* 44: 3109–3118.
74. Matthes, F., M. M. Hettich, J. Schilling, D. Flores-Dominguez, N. Blank, T. Wiglenda, A. Buntru, H. Wolf, S. Weber, I. Vorberg, et al. 2018. Inhibition of the MID1 protein complex: a novel approach targeting APP protein synthesis. *Cell Death Discov.* 4: 4.
75. Muri, J., S. Heer, M. Matsushita, L. Pohlmeier, L. Tortola, T. Fuhrer, M. Conrad, N. Zamboni, J. Kisielow, and M. Kopf. 2018. The thioredoxin-1 system is essential for fueling DNA synthesis during T-cell metabolic reprogramming and proliferation. *Nat. Commun.* 9: 1851.
76. Sag, D., D. Carling, R. D. Stout, and J. Suttles. 2008. Adenosine 5'-monophosphate-activated protein kinase promotes macrophage polarization to an anti-inflammatory functional phenotype. *J. Immunol.* 181: 8633–8641.
77. Kim, B., H. Y. Kim, B. R. Yoon, J. Yeo, J. In Jung, K. S. Yu, H. C. Kim, S. J. Yoo, J. K. Park, S. W. Kang, and W. W. Lee. 2022. Cytoplasmic zinc promotes IL-1β production by monocytes and macrophages through mTORC1-induced glycolysis in rheumatoid arthritis. *Sci. Signal.* 15: eabi7400.
78. Cheng, Y., M. Mao, and Y. Lu. 2022. The biology of YAP in programmed cell death. *Biomark. Res.* 10: 34.
79. Zhang, X., A. Abdelrahman, B. Vollmar, and D. Zechner. 2018. The ambivalent function of YAP in apoptosis and cancer. *Int. J. Mol. Sci.* 19: 3770.
80. LeBlanc, L., B. K. Lee, A. C. Yu, M. Kim, A. V. Kambhampati, S. M. Dupont, D. Seruggia, B. U. Ryu, S. H. Orkin, and J. Kim. 2018. Yap1 safeguards mouse embryonic stem cells from excessive apoptosis during differentiation. *Elife* 7: e40167.
81. Kim, H. J., S. B. Song, Y. Yang, Y. S. Eun, B. K. Cho, H. J. Park, and D. H. Cho. 2011. Erythroid differentiation regulator 1 (Erdr1) is a proapototic factor in human keratinocytes. *Exp. Dermatol.* 20: 920–925.
82. Lee, J. H., C. H. Kim, D. G. Kim, and Y. S. Ahn. 2009. Microarray analysis of differentially expressed genes in the brains of tubby mice. *Korean J. Physiol. Pharmacol.* 13: 91–97.
83. Ma, S., Z. Meng, R. Chen, and K. L. Guan. 2019. The Hippo pathway: biology and pathophysiology. *Annu. Rev. Biochem.* 88: 577–604.
84. Petzold, J., and E. Gentleman. 2021. Intrinsic mechanical cues and their impact on stem cells and embryogenesis. *Front. Cell Dev. Biol.* 9: 761871.
85. Yu, F. X., B. Zhao, and K. L. Guan. 2015. Hippo pathway in organ size control, tissue homeostasis, and cancer. *Cell* 163: 811–828.
86. Meng, K. P., F. S. Majedi, T. J. Thauland, and M. J. Butte. 2020. Mechanosensing through YAP controls T cell activation and metabolism. *J. Exp. Med.* 217: e20200053.

87. Zuo, E., Y. J. Cai, K. Li, Y. Wei, B. A. Wang, Y. Sun, Z. Liu, J. Liu, X. Hu, W. Wei, et al. 2017. One-step generation of complete gene knockout mice and monkeys by CRISPR/Cas9-mediated gene editing with multiple sgRNAs. *Cell Res.* 27: 933–945.
88. Rhie, A., S. Nurk, M. Cechova, S. J. Hoyt, D. J. Taylor, N. Altemose, P. W. Hook, S. Koren, M. Rautiainen, I. A. Alexandrov, et al. 2023. The complete sequence of a human Y chromosome. *Nature* 621: 344–354.
89. Stampouloglou, E., N. Cheng, A. Federico, E. Slaby, S. Monti, G. L. Szeto, and X. Varelas. 2020. Yap suppresses T-cell function and infiltration in the tumor microenvironment. *PLoS Biol.* 18: e3000591.
90. Wang, Y., and S. Perlman. 2022. COVID-19: inflammatory profile. *Annu. Rev. Med.* 73: 65–80.
91. Wong, L. R., and S. Perlman. 2022. Immune dysregulation and immunopathology induced by SARS-CoV-2 and related coronaviruses—are we our own worst enemy? *Nat. Rev. Immunol.* 22: 47–56.